THE LINK BETWEEN GUT MICROBIOTA METABOLISM AND HOST GLUCONEOGENESIS BY VASOACTIVE INTESTINAL PEPTIDE

A Thesis
Submitted to the Graduate Faculty
of the
North Dakota State University
of Agriculture and Applied Science

By

Razia Dawlaty

In Partial Fulfillment of the Requirements
for the Degree of
MASTER OF SCIENCE

Major Program:
Microbiology

August 2022

Fargo, North Dakota

North Dakota State University
Graduate School

Title

The Link between Gut Microbiota Metabolism and Host Gluconeogenesis by Vasoactive Intestinal Peptide

By

Razia Dawlaty

The Supervisory Committee certifies that this ***disquisition*** complies with North Dakota State University's regulations and meets the accepted standards for the degree of

MASTER OF SCIENCE

SUPERVISORY COMMITTEE:

Glenn Dorsam, PhD
Chair

Jane Schuh, PhD

Colbert Christopher, PhD

Penelope Gibbs, PhD

Sheela Ramamoorthy, PhD

Approved:

9-6-2022
Date

John McEvoy, PhD
Department Chair

ABSTRACT

The gut microbiota (GM) plays a beneficial role in host metabolism. In mammals, the GM ferments dietary fiber into short chain fatty acids (SCFA), like propionate, that improves glucose metabolism. Rats fed a propionate diet increased intestinal gluconeogenic (IGN) gene expression, which was blocked by treatment with the neurotoxin, capsaicin, suggesting a neuronal-dependent mechanism. We hypothesized that the gut neuropeptide, vasoactive intestinal peptide (VIP), links GM derived propionate to IGN expression. We fed VIP deficient mice a 5% propionate chow diet (n=60) for 2 weeks and measured mRNA levels for GN genes by dPCR. Basel intestinal and liver GN mRNA expression was dysregulated by the loss of VIP. GN mRNA levels in liver were differentially altered in males versus females fed a propionate diet in a VIP-dependent manner. We conclude that VIP regulates basal intestinal and hepatic GN mRNA expression and mediates propionate induced GN mRNA changes in liver.

ACKNOWLEDGMENTS

I would like to express my appreciation and gratitude to my primary advisor Dr. Glenn Dorsam for supporting me and giving me the opportunity to be his graduate student. Thank you, Dr. Dorsam, for your guidance and your support over the last two years of my research. Life is always challenging, especially for a mom with three children, but my advisor didn't let me fail. I would like to thank Justin Daniels, our previous lab manager, for his guidance and helping. Thank you, Emma Hawley, for always being very friendly and kind. Thanks to all who worked in Dr. Dorsam's lab in the last two years; Dr. Dorsam's lab members were very friendly and supportive. I would like to express my appreciation to our department core director, Scott Hoselton, for his technical support and help. Mr. Scott is a very nice, kind, and friendly person, I always felt welcomed when I needed help. I would like to express my appreciation to my committee members Dr. Colbert Christopher, Dr. Penelope Gibbs, Dr. Jane Schuh, and Dr. Sheela Ramamoorthy for their support and guidance through my graduate career. A special thanks to Dr. John McEvoy, the Microbiological Science department chair who opened the door for me to be in the department for my master's degree. Thanks to everyone else in the department, especially to the Administrative Secretary Jerie Little, who always helped me with shipping and room reservations.

DEDICATION

I dedicate my education and my work to my father, who was the only one who supported my sisters and me and let us to go to school in a very toxic environment against woman education. I would like to dedicate my accomplishments to my husband, who has always tried the best to support his family by working hard. I have never worried financially since my husband was the one to support his family. If my husband didn't support me, it would not have been possible to quit my full-time job at Aldevron and go back to school to work on my MS. Thanks Fawad Dawlaty for being an amazing husband and father for your wife and your three daughters. My three daughters Ranna 19, Hosna 15, and Sana 8 years old are great and responsible kids. For most of the time, I felt like I am with my three best friends. Ranna gave me the opportunity to study and stay longer in the lab by babysitting and giving rides to her siblings. Hosna doing great at school helped me to take care of her little sister with babysitting. Sana always brought happiness to me by smiling and hugging me. Each of my daughters had a role in reaching my goal, and I am very grateful and proud of them. I would like to thank my sister Dr. Marziah Hashimi, who always encouraged and supported my education.

TABLE OF CONTENTS

LIST OF TABLES

LIST OF FIGURES

LIST OF ABBREVIATIONS

AA.....Amino Acid

ADHD.....Attention Deficit Hyperactivity Disorder

BMI.....Body Mass Index

CREB.....cAMP Responsive Element Binding Protein

dPCR.....Digital PCR

DS.....Double-Stranded

ECL.....Extra-Cellular Loop

FBP1.....Fructose 1,6BiPhosphotase

GPCR.....G-Protein Coupled Receptor

GIP.....Gastric Inhibitory Polypeptide

GIT.....Gastrointestinal Tract

G6phase.....Glycose 6 Phosphatase

GLUT2.....Glucose Transporter 2

HET.....Heterozygous

IBD.....Inflammatory Bowel Disease

ICL.....Intra-Cellular Loop

IGN.....Intestinal Gluconeogenesis

MIP-2.....Macrophage Inflammatory Proein-2

KO.....Knock Out

LB.....Luria-Bertani

MALT..... Mucosa-Associated Lymphoid Tissues

NO.....Nitric Oxide

N-ted.....N-Terminal Ectodomain

qPCR.....Quantitative PCR

PACAP.....Pituitary Adenylate Cyclase Activation Polypeptide

PCK1.....PhosphoEnol Pyruvate Carboxy Kinase

PCX.....Pyruvates Carboxylase

PCR.....Polymerase Chain Reaction

PHM.....Peptide Histidine Methionine

PHI.....Peptide Histidine Isoleucine

PNS.....Peripheral Nervous System

VIP.....Vasoactive Intestinal Peptide

VPACl/2.....Peptide/Pituitary Adenylate Cyclase Activating Polypeptide Receptor1/2

SCFA.....Short Chain Fatty Acid

SOC.....Super Optimal broth with Catabolites repression

SS.....Single Stranded

Taq.....Thermus Aquaticus

TJ.....Tight Junctions

WHO.....World Health Organization

WT.....Wide Type

1. VASOACTIVE INTESTINAL PEPTIDE

1.1. Background

Vasoactive intestinal peptide (VIP) is a neuropeptide that is 28 amino acids (AA) in length (3.3 kDa). VIP was discovered from swine intestine and was named for its vasodilatory role when added to arterioles as reported by Drs. Said and Mutt in 1970. (Said and Mutt,.1970). VIP is widely expressed in the central nervous system (CNS) and is delivered by the peripheral nervous system (PNS) to many primary and secondary immune organs, including the mucosa-associated lymphoid tissues (MALT) of the pulmonary and gastrointestinal tract (GIT), thymus, spleen, and bone marrow (Ericsson and McAdams 2022). VIP belongs to the secretin/glucagon superfamily that regulates circadian rhythm activities, intestinal gut microbiota homeostasis and immunity (Colwell, et al.,2003; Bains et al.,2019). The secretin/glucagon family contains 15 different small peptides that share similar and distinct biological activities. There is evidence that this superfamily began with an exon duplication from a PACAP-like gene and continued to expand with additional gene duplications as invertebrates evolved into vertebrates. The ancestor of this superfamily, PACAP, is the most conserved peptide at the primary sequence within this superfamily (Sherwood et al., 2000). All 15 superfamily peptides, have the following common properties: 1) 27-44 AA in length; 2) co-expressed within the endocrine, immune and nervous systems, 3) possession of alpha-helices in their secondary structure; 4) N-terminal Cap structures (**See Table.1**), (Couvineau et al., 2012). Several of these peptides bear a carboxy-terminal amide including secretin and VIP. The human VIP gene is located on position 25.2 on chromosome 6 and in rodents on the syntenic region of chromosome 10 (Dorsam et al., 2011). The N-terminal part of VIP plays a crucial role in selectively recognizing its GPCR receptors, and the alpha helical structure in the C-terminus of the VIP ligand is important in receptor crosslinking

(Ceraudo et al., 2008)) VIP degrades rapidly *in vivo* with a half-life of less than 1 min due to protease activity (Hassan et al., 1994).

Table 1. List of all 15 peptides from the secretin/glucagon superfamily and PHI with their AA sequences and peptide lengths

Peptide	**Amino Acid Sequence**	**# AA**
VIP	HSDAV FTDNY TRLR KQMA VKKY LNSI LN	28
PACAP-27	HSDGI F TDSY SRYR KQMA VKKY LAAV L	27
PACAP-28	HSDGI F TDSY SRYR KQMA VKKY LAAV LGK RYKQ RVKN K	38
Helodermin	HSDAI F TEEY SKLL AKLA LQKY LASI LGSR TSPP P	35
PHM	HADGV F TSDF SKLL GQLS AKKY LESL M	27
Secretin	HSDGT F TSEL SRLR EGAR L QRLL QGLV	27
GRF	YADAI F TNS YRK VLG QLS ARK LLQ DIM SRQ QGE SNQ ERG ARA ER	44
Glucagon	HSQGT F TSD YSK YLD SRR AQD FVQ WLM NT	29
GLP-1	HAEGT F TSD VSS YLE GQA AKE FIV WLV KGR	30
GLP-2	HADGS F SDE MNT ILD NLA ARD FIN WLI QTK ITD	33
GIP	YAEGT F ISDY SLAM DKIH QQDF VNWL LAQK GKKN DWKHNITQ	42
PTH	SVSE IQLM HNLG KHLN SMER VEWL RKKL QDVH NF	34
PTHrp	AVSEH QLLH DKGK SIQK LRRR FFLH HLIA EIHT A	34
Calcitonin	CGNLS TCML GTYT QDFN KFHT FPQT AIGV GAP	32
CRF	SEEPP ISLD LTFH LLRE VLEM ARAE QLAQ QASH NRK LMEI I	41
PHI	HADG VFTS DYSR LLGQ ISAK KYLE SLI	27

1.2. The Central Dogma Specifics for the VIP Gene

The human VIP gene has seven exons that is interrupted by six introns and spans 9 kb. This gene is initially translated into a 170 AA prepropeptide and proteolytically cleaved to generate at least two biologically active peptides, called VIP and phenylalanine histidine methionine (PHM). Exon five encodes the entire VIP protein primary structure (e.g., 28 AA), while exon four encodes PHM (e.g. 27 # of AA) (Dorsam, et al. 2011). The primary AA sequence for VIP is identical in most mammals, including human, cow, pig, goat, dog, and rat

(Gastone and Malendowicz, 1998). The VIP gene is similar in mouse and human according to its gene organization with a total of 7 exons, however exon 4 encodes Peptide Histidine Isoleucine (PHI-27) in rodents that is an analog to human PHM-27. VIP is 68% identical at the primary AA sequence level to another secretin family peptide called pituitary adenylate cyclase activating polypeptide (PACAP), (See Figure1). There are two forms or Isofrom of PACAP. The first is 38 AA in length and the second is 27 AA in length (Dorsam, et al., 2011). A VIP knockout (KO) mouse strain was generated in 2003 by homologous recombination of exons 4 and 5 being disrupted by inserting a neomycin resistance DNA cassette. These mice were used to collect seminal observations regarding circadian oscillation defects that was the first report to provide evidence that VIP influences diurnal rhythms (Colwell, et al., 2003). It is noteworthy to mention that both VIP (exon 5) and PHM (exon 4) were simultaneously disrupted in the VIP KO mouse strain and therefore this genetically altered mouse strain was null for both peptides (See Fig. 1).

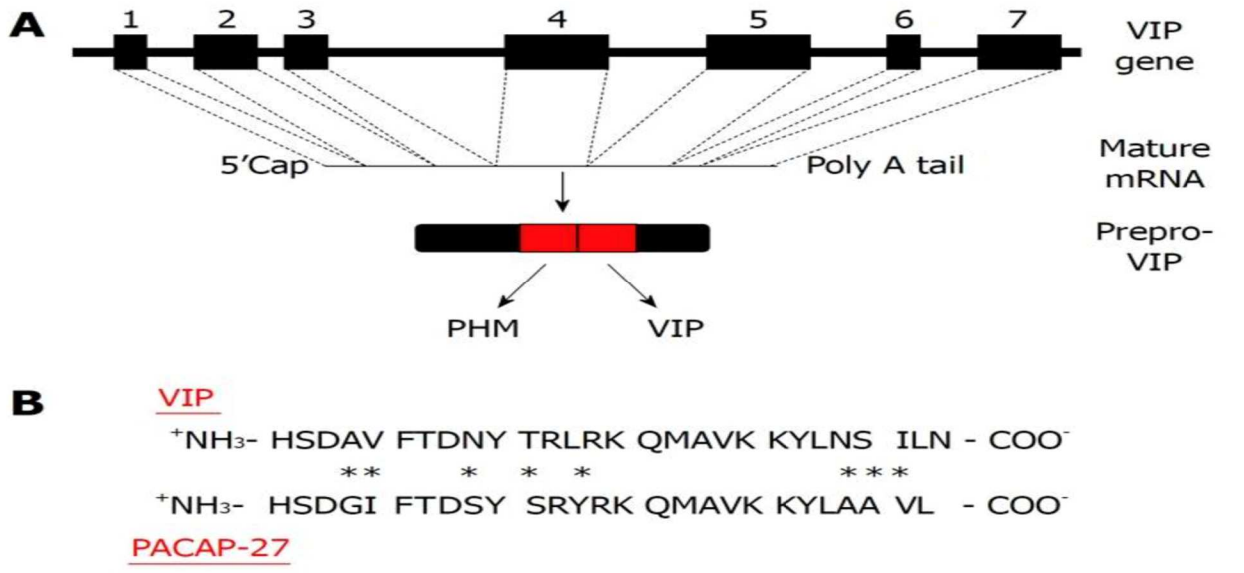

Figure 1. **Summary of the Central Dogma for the VIP gene**. A. The VIP gene spans 9 kb and contains seven exons and six introns. The VIP gene is initially translated into a 170 AA prepropeptide followed by proteolytically cleaving into two biologically active peptides, VIP and PHM/PHI. The coding sequence for the VIP protein is located within exon 5, while exon 4 encodes PHM/PHI. B. Comparison of AA sequences between VIP and PACAP, with asterisks representing the difference.

1.3. VIP Receptors

VIP has at least three endogenous receptors. Two high-affinity receptors are vasoactive intestinal peptide/pituitary adenylate cyclase activating polypeptide receptor 1 (VPAC1) and VPAC2. These two G-protein-coupled receptors (GPCR) are members of the secretin/glucagon receptor family that bind to VIP and PACAP with equal affinity (Kd ≈ 1 nM) (Hirabayashi et al., 2018). A third low-affinity GPCR is called, pituitary adenylate cyclase activating polypeptide receptor 1 (PAC1), that has a 1000-fold lower affinity for VIP, but binds PACAP with similar affinity to VPAC1 and VPAC2(Hirabayashi, Hanamachi, and Shioda 2012). In summary, PAC1 is more selective as it preferentially ligates PACAP compared to VIP, while VPAC1 and VPAC2 are non-selective as they bind both VIP and PACAP with equal affinity. PAC1 is expressed in the brain and adrenal medulla, while VPAC1/ VPAC2 are expressed in the brain and several peripheral tissues including liver, lung, pancreas, stomach, heart, bone, immune cells, kidney, and gastrointestinal and reproductive tracts (Xie, Geng el 2022). VPAC1 receptor expression is found the central nervous system (CNS) within certain regions, including the supraoptic nucleus, pineal gland, the putamen and pyriform cortex. VPAC2 receptor in expressed in the CNS, and found in the suprachiasmatic nucleus, amygdala, hypothalamus, periventricular nucleus, cerebral cortex and in the thalamus. As was mentioned above, all three VIP/PACAP GPCRs activate signaling through Gαs activation of adenylyl cyclase (e.g. the enzyme that catalyzes cAMP production from ATP). As was mentioned above, PAC1 receptors found mostly in the brain have low affinity to VIP, and therefore PAC1 is not considered a primary physiological receptor for VIP. Importantly, VIP is more active in peripheral tissues rather than the brain (Aaron C et al., 2022). The extracellular domains (See Fig. 2) of VPAC1/VPAC2 receptors contain conserved AAs that are crucial for VIP binding and these conserved AA residues are poorly conserved in

other members of the class B GPCR. In contrast, these two receptors are distinct from each other by AA sequence and structure -function relationship (Nicole et al., 1997). The primary AA sequence between human VPAC1 and VPAC2 is 49%. Both GPCRs have tissue distribution complementarity, where tissues that express VPAC1, VPAC2 receptor expression is typically absent, and the converse. (Usdin, et al., 1994).

1.3.1. GPCR

GPCRs were discovered by two physiologists Alfred Gilmna and Martin Rodbell, and both were awarded the Noble Prize in 1994 for their scientific contributions in the GPCR field. Their research was an extension of early studies started by several biochemical and biophysical investigators in the late 1980s. GPCRs are membrane receptors that regulate physiology and cellular functions in all organs. To date, there are approximately 800 different GPCR genes discovered in the human genome (Robilka and Lefkowitz 2013). This receptor family possesses a 7-transmembrane structure with three extracellular loops (ECL-3), three intracellular loops (ICL-3), an N-extracellular ectodomain (N-ted), and an intracellular C-terminus region. The heterotrimeric G protein complex that interacts with the C-terminus region is composed of an alpha, beta, and gamma subunit that mediates intracellular signaling (**See Fig. 2**).

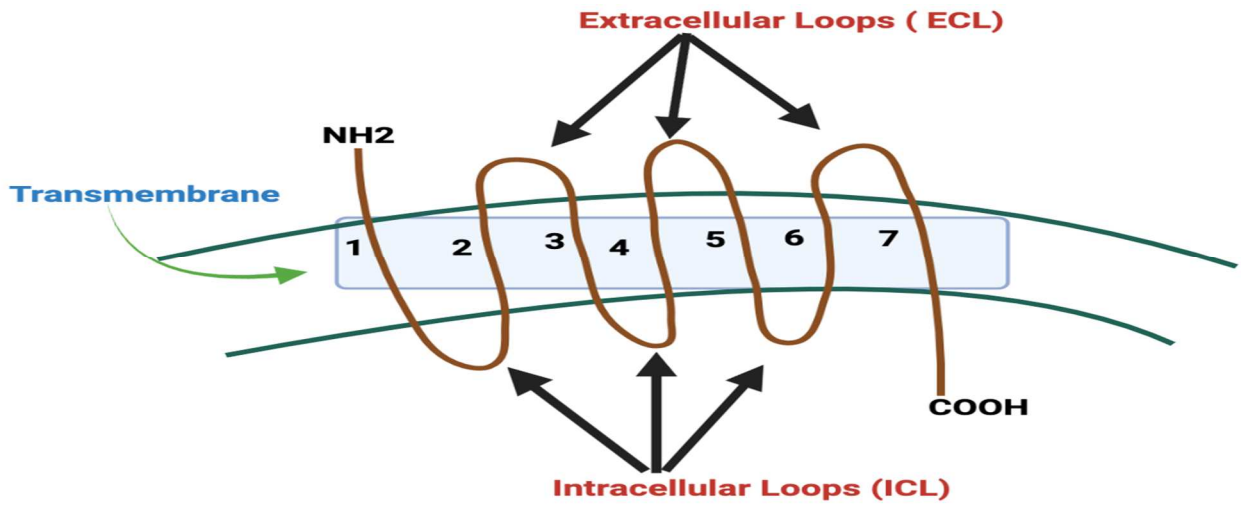

Figure 2. **Structure of GPCR receptor on the plasma membrane**. These receptors consist of a 7- transmembrane domain structure that "snakes" through the plasma membrane 7 times, with three extracellular loops, three intracellular loops, N-extracellular ectodomain and intracellular C-terminus as indicated.

Based on physiological and structural activities, GPCRs have been classified into five major families (rhodopsin, adhesion, secretin, glutamate, and frizzled) and four classes (A, B, C, and F). The rhodopsin, class A family is the largest among these five, and it has various functions pertaining to immunity, vision, and olfaction. The secretin family is classified as a class B family and is comprised of 47 receptors, with 15 of these belonging to the secretin/glucagon superfamily. The glutamate family is a class C family, and it consists of 15 receptors that are involved in synaptic transmission. The Class F family is made up of 11 receptors that do not have significant sequence homology across families. Therefore, the seven transmembrane domains observed in all GPCRs are conserved among the five families (Belfiore and LeRith "Principle of Endocrinology and Hormone Action").

The class B receptor indicates very low sequence homologies with other GPCR classes (Laburthe et al., 2007). Class B receptors have several significant characteristics, including a large (>120 AA residues) and structured N-ted. The N-ted possesses six highly conserved cysteine residues that make three disulfide bridges, which is significant in class B GPCR ligand

binding and specificity (Couvineau et al., 2012). The N-ted of class B receptor indicates the major binding site for its related peptide ligands.

1.3.2. VPAC1 Receptor

The mouse VPAC1 (Vipr1) gene was discovered in 1992 and is located on chromosome 9 (Ishihara et al.1992). The mouse VPAC1 gene is made up of 13 exons and 12 introns (Hashimoto et al., 1999). This gene encodes for a 459 AA glycosylated protein that is ≈50% identical with the rat PAC1 receptor (Dorsam, Benton, et al., 2012). The glycosylated N-ted domain of the VPAC1 receptor has an essential role in VIP recognition and binding. Evidence for this was reported by a study that demonstrated a physical contact between the VIP ligand and the side chains of the N-ted of the VPAC1 receptor (Nicole et al., 1997) This binding mechanism has two advantages. First, the VIP ligand has high affinity for its receptor under physiological conditions of approximately nanomolar range. Second, the VIP ligand can interact with the glycosylated receptor, which is particularly crucial for ligand specificity. (Couvineau, Ceraudo, el al.,1996).

VPAC1 is highly expressed in the gastrointestinal (GI) tract where it mediates VIP and PACAP effects on gut homeostasis. VPAC1 signaling also transmits anti-inflammatory effects in various immune and non-immune cells within the GI tract. The first VPAC1 KO mouse was generated in 2010 using embryonic stem cells by removing exons 4-6 that resulted in a VPAC1-null mouse for the investigation into intestine, pancreatic and immune function (Fabricius, Karacay, et.al., 2011, **See Fig. 3**).

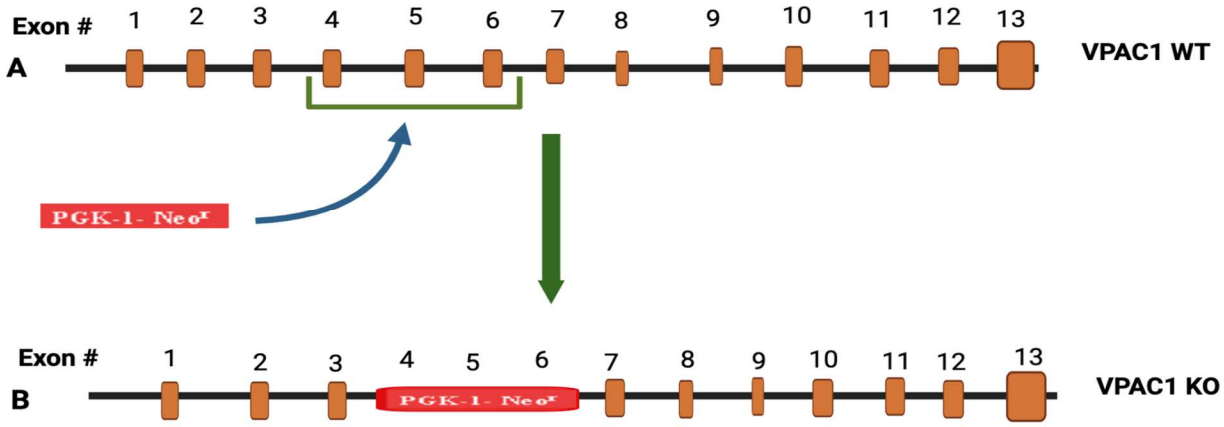

Figure 3. **Knockout strategy** A) VPAC1 WT gene with numbered exons as orange rectangular boxes. B) VPAC1 KO gene with exon 4-6 ejected with the insertion of a neomycin cassette.

1.3.3. VPAC2 Receptor

The mouse VPAC2 (Vipr2) gene was discovered in 1993 in a rat pituitary gland cDNA library and is located on chromosome 12. The VPAC2 gene contains 13 exons and 12 introns. The rat and human VPAC2 receptors consist of 437 and 438 AA, respectively. The first VPAC2 KO mouse was generated in 2002 in mouse embryonic stem cells by homologous recombination that resulted in the replacement of exon 1 by the lacZ cDNA to study the circadian rhythm cycle (Harmar et al., 2002, **See Fig. 4**). These seminal studies clearly demonstrated that VIP was a master circadian regulator, and its molecular action was transmitted by VPAC2 signaling within the suprachiasmatic nucleus (SCN) within the brain. The N-terminal extracellular domain of VPAC2 receptor containing the AA, glutamate 24 and isoleucine 31, are involved in ligand binding (Nicole et al., 1997). VPAC2 has an extra Proline residue in position 280 at EC2, which VPAC1 receptor is shorter by one AA and lacks a proline at 294 positions. Studies have shown that threonine 274 and proline 280, that are not involved in ligand recognition by the VPAC1 receptor, are essential for VPAC2 binding to ligand (Vertongen et al., 2001).

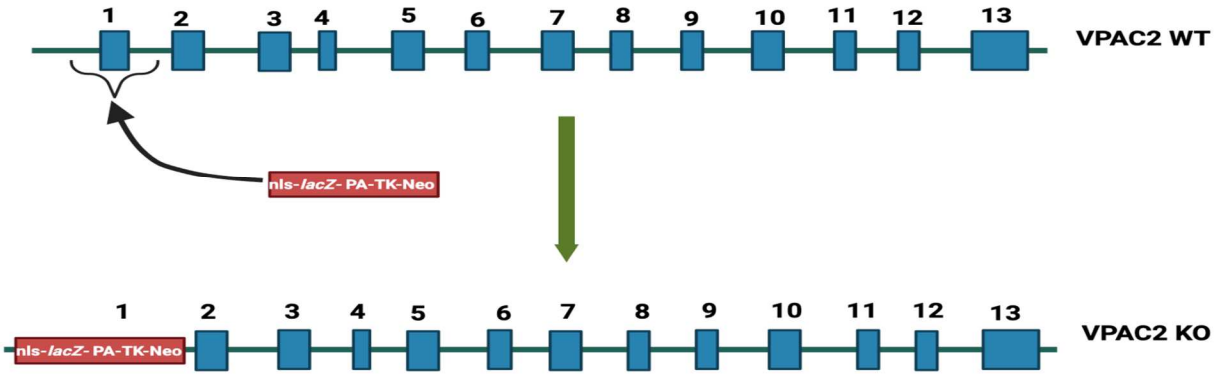

Figure 4. **Knockout Strategy**. A) VPAC2 WT gene with numbered exons as blue rectangular boxes B) VPAC2 KO genes with exon 1 swapped out and inserted with a neomycin cassette.

1.4. Biological Activities of VIP Signaling

VIP has been investigated since 1970 after its discovery by Drs. Said and Mutt, while the VIP receptors were discovered in the 1990s. VIP has a wide range of biological activities and is expressed in different tissues, including the central and peripheral nervous system consistent with its classification as a neurotransmitter. VIP is a potent vasoactive factor that dilates arterioles when added exogenously to them in *ex vivo* experiments. VIP mediates vasodilation action through binding to both receptors VPAC1 and VPAC2.Vasodilator action of VIP involves the contribution of nitric oxide (NO) as inhibition of NO synthesis caused in the abatement of VIP induced vasodilation of endothelium in sheep meddle cerebral arteries (Gaw et al,. 1991). In porcine basilar arteries, VPAC1 is expressed on the endothelium and VPAC2 receptor expressed on the outer layer of smooth muscle that surrounds the artery. VIP mediated vasodilation through VPAC1 is mediated by inducing nitric oxide (NO) synthesis into blood, while VPAC2 induces vasodilation by inducing relaxation via the cAMP pathway in smooth muscle cells. (Grand and Wadsworth et al., 2006).

Signaling through the VPAC2 receptor, VIP acts as a master circadian regulator. Evidence for this was first reported in 2002 that showed VPAC2 signaling was imperative for

circadian function in mice. A year later, Colwell et al., generated a VIP/PHI deficient mouse strain and confirmed VIP as a master circadian regulator. They observed that deletion of VIP or VPAC2 caused a cycling shift in wake/sleep cycles, reduced food intake and a loss of body weight Harmar *et al.*, 2002 add Colwell too). Moreover, VPAC2-null mice failed to express the clock-controlled gene arginine vasopressin (AVP) and the circadian core clock genes: mPer1, mPer2, and mCr1in the CNS (Harmer et al,.2002). The term 'circadian' is derived from the Latin 'circa' (around) and 'dies' (day). The body clock oscillates with an internal period of 24 hours, and it entrains when it receives enough daily corrective signals from the environment, such as daylight (e.g., photons received by the optic nerve called photonic information). The circadian rhythm is a natural process that controls the physical, mental, and behavioral changes during a 24-hour period within an organism. An example of a light related circadian rhythm is the natural sleeping at night (diurnal) or sleeping during the daylight (nocturnal). The central circadian rhythm within the brain regulates all systemic biological clocks. Biological clocks consist of proteins that communicate within cells and throughout the body. Similar genes that make the clocks molecular components are found in human, fruit-flies, mice, plants, fungi and other organisms, making this an ancient biological function. In the brain, a master clock represents a group of 20,000 nerve cells that control all systemic clocks in a living organism. The suprachiasmatic nucleus located within the hypothalamus makes up the master clock (Circadian Rhythms, 2017)

VIP is anti-inflammatory and has been extensively studied in human inflammatory disorders, including inflammatory bowel diseases (IBD). In IBD patients, some reports have reported a reduction in the expression levels of VIP and its receptors that were negatively correlated with the extent of inflammation (Jayawardena et al., 2017). Additional anti-

inflammatory effects by VIP is the regulation of inflammatory cytokines, such as IFN-γ and IL-1, while elevating the anti-inflammatory cytokine, IL-10 (Delgado et al., 2004, Anderson et al., 2010) In innate immunity, VIP reduces the expression of macrophage and monocyte proinflammatory cytokines such as IL6, IL8, IL18, and macrophage inflammatory protein-2 (MIP-2). In adaptive immunity, VIP downregulates the expression of T-cell-derived proinflammatory cytokines such as IL-2, IL-4, IFN-γ and TNF-alpha, while it upregulates the expression of anti-inflammatory cytokines IL-10 in B cells and inflammatory mediators, like IL-22 in ILC3 (Xie et al.,2013). VIP also downregulates the co-stimulatory molecules on dendritic cells in lamina propria of the GIT (Toscano et al.,2010), that further diminishes T cell effector activation.

1.4.1. VIP Activities in the Intestinal Tract

VIP is a gut peptide that has a crucial role on intestine homeostasis. Studies have demonstrated the importance of this peptide on gut physiology by regulating gastric acid secretion and water absorption in the large intestine. VIP plays a vital role on intestinal barrier by regulating mucus secretion and upregulation of tight junction (TJ) proteins, as well as epithelial cell proliferation and survival. The GI tract is one of the most exposed systems to the external environment, including pathogenic chemicals and microorganisms, and the intestinal barrier is the first defense against these pathogenic agents. The chemical layer of the intestinal barrier consists of several factors that provide a first line of defense, called mucus. This substance is released by intestinal epithelial cells that beneficially separates bacteria from intestinal epithelial cells thus preventing them from contacting the intestinal epithelial cell layer and causing unwanted inflammatory reactions. AN important mucus protein, which makes up a significant percentage of the mucus layer, is MUC2 and is secreted by goblet cells, a type of intestinal

epithelial cell. In human colonic epithelial cells, VIP activates MUC2 transcription via a cAMP signaling pathway activating the ERK and p38 MAP kinases (Hokari et al., 2005). Another study reported that VIP deficient mice demonstrated that goblet cell numbers declined along with reduced MUC synthesis and secretion (Wu et al., 2015). The physical barrier of the intestine is a single intestinal epithelium layer that expresses intercellular TJ proteins, such as claudine and occludin that acts like a wall. Several studies have reported that VIP was decreased during intestinal barrier damage that was associated with reduction of TJ. VIP administration rescued this phenotype. (Xie et al., 2022). Propionate activates intestinal gluconeogenic genes (IGN), like G6Pase, through the secretion of neuronal VIP that binds to VPAC1 (De- Vadder et al., 2015). VIP is crucial for gut microbiota diversity and composition via its VPAC1 receptor in male and female mice. VIP deficient mice were associated with having decreased gut microbiota diversity and significant compositional changes compared to wild type mice through an unknown mechanism. (Manpreet et al., 2019).

2. SEQUENCE VALIDATION OF GENOTYPING PCR PRODUCTS FOR VIP AND ITS RECEPTORS, VPAC1 AND VPAC2

2.1. Background

Genotyping is an essential step for knockout mouse research projects because it determines the genetic identity of mice being employed as: wild type (WT), heterozygous (HET; mutant carrier on one allele) or homozygous (KO, mutant for both alleles). Research in the Dorsam laboratory utilizes three different mouse strains, including the neuropeptide VIP, and its two cognate GPCRs termed VPAC1 and VPAC2. To date, our genotyping assays interrogated the presence of either a WT or KO allele by polymerase chain reaction (PCR) and visualized expected sized PCR products by agarose gel electrophoresis stained with a fluorescent dye (ethidium bromide or EZ vision) as previously published by others (Colwell et al., 2003; Fabricius et al., 2011; Harmar et al., 2002)). However, the sequence identity has not yet been confirmed by our research group. To this end, I started my first project in the Dorsam lab with the objective of confirming the sequence identity of all six relevant PCR products (3 WT and 3 KO PCR species) for the three mouse strains mentioned above. This work employed the following strategy: (1) Mouse tail biopsy collection , (2) PCR genotyping analysis using sequence-specific primers for VIP, VPAC1 and VPAC2 genes, (3) PCR products separated by agarose electrophoresis, (4) PCR DNA species of interest excised from agarose gels with a razor blade, (5) PCR products subcloned into the Topo cloning expression vector®, (6) subcloned vector transformed into competent M13 *E. coli* bacteria, (7) overnight culture of a single bacteria colony selected with ampicillin, (8) plasmid DNA isolation by spin column chromatography, (9) restriction enzyme digestion with EcoR1 to confirm presence of the expected PCR sized

product, (10) and DNA sequencing by Sequetech Corporation (**See Fig. 5**). DNA sequence data was BLASTED using the NCBI nucleotide alignment.

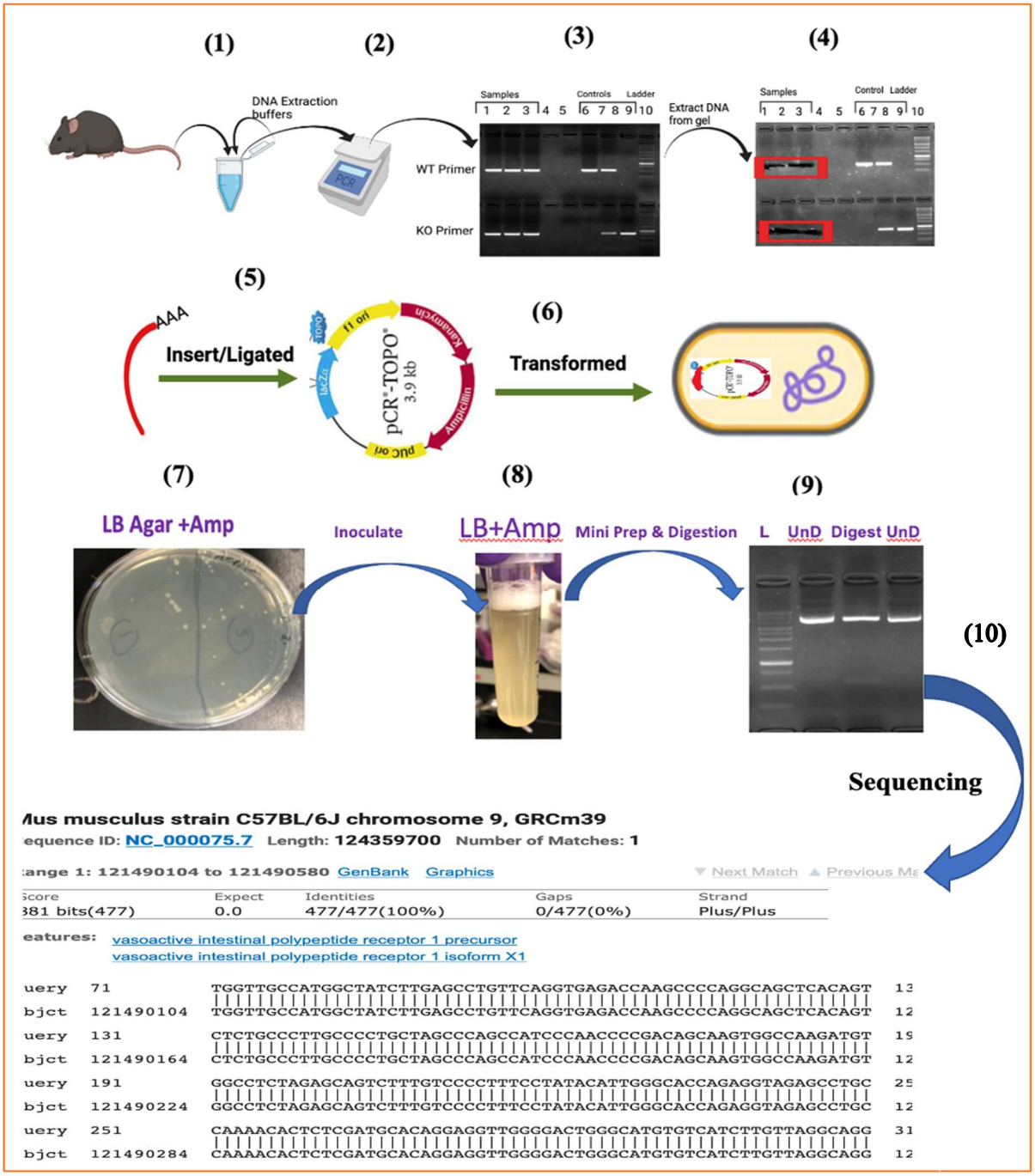

Figure 5. **Summary of experimental strategy for subcloning and sequencing all six relevant DNA sequences.**

2.1.1. Polymerase Chain Reaction (PCR)

PCR represents a biochemical reaction catalyzed by a heat-stable enzyme that was first used to amplify deoxyribonucleic acid (DNA) in 1985 by biochemist Kary Mullis, for which he won the Nobel Prize for this discovery in 1993. This revolutionary technique amplifies a single DNA molecule a million-fold (Lorenz, 2012). Today, PCR is one of the most important techniques in modern molecular biology. It is widely used in all molecular research such as diagnostic, forensic science, plant science, and biomedical laboratories, to name a few. To distinguish between different mouse genotypes, PCR is a powerful tool for identifying mice genotypes. PCR has three stages, where the second stage is repeated multiple times during the amplification process. The other two, sometimes optional, stages depend on the specific kind of taq-polymerase used. The first stage of the PCR reaction is a single step that requires 94°C-96°C for 2-20 min that serves at least two purposes. The primary purpose is to activate the Thermus aquaticus (taq)-polymerase enzyme that is typically bound to a heat-labile antibody rendering it enzymatically inactive, called hot start, but becomes active after antibody denaturation. The second purpose of the first stage of PCR is to denature all DNA templates from double-stranded (ds) DNA molecules to linear, single-stranded (ss) DNA molecules with little to no secondary structure. The second stage involves three different temperature-controlled steps representing (1) denaturation, (2) annealing and (3) extension. The first step is to denature dsDNA to ssDNA at 93°C -95°C in a similar way to the first initial stage but is usually for a shorter time on the range of seconds rather than minutes. The second step of stage two drops the temperature to between 55°C to 65°C to allow for short oligonucleotide primers to anneal to the DNA template (e.g., “book-ending” the DNA segment of interest that is to be amplified). The final step of stage two increases the temperature to 72°C, which allows for maximal extension of DNA amplification

(e.g., complementary chain elongation) as the Taq-polymerase is most active at this temperature. Stage two is repeated up to 40 times, called cycles, to amplify the PCR product millions of times from a few starting DNA templates. The third and final stage is a single step that maintains the extension temperature of 72°C for 5-10 min to ensure for complete DNA extension of PCR products as well as ensuring for the addition of a single adenine nucleotide overhang at the end (e.g., 3' prime end) of each newly synthesized DNA species. This latter event of 3' adenine overhangs is important for subcloning PCR products into sequencing/expression vectors (Bio-Rad, 5362) (**See Fig. 6**).

PCR has five important and essential ingredients that are required to perform a reaction and each of these ingredients has its own role and importance. First, short sequence-specific ssDNA primers (18-22 bp oligonucleotides) that hybridize to the target template. These sequence-specific primers are complementary to either one of the two DNA strands, called forward (5') and reverse (3') primers, that act in initiating chain elongation catalyzed by Taq-polymerase. Second, all four deoxyribonucleic nucleotides or dNTPs that represent the substrates for Taq-polymerase (e.g., building blocks of DNA) and are abbreviated as A (adenine), G (guanine), T (thymine), and C (cytosine) are included. These four dNTPs are needed for synthesis of new DNA molecules. Third, Taq-polymerase is a heat-stable DNA polymerase originally isolated from thermophilic bacteria that function at extreme temperatures, 70°C to 75°C, and remain enzymatically active as high as 96°C. Taq is abbreviated from Thermus aquaticus, with Thermus used for being stable at high temperature and aquaticus because it was found in water. Taq-polymerase catalyzes complementary chain elongation by "reading" the DNA template and adding the appropriate nucleotide to generate a Watson/Crick bp in a 5'→ 3' direction initiated at the position of the primer (**See Fig. 7**). Fourth, a buffer (pH 8.0) that

provides a suitable environment for Taq-polymerase that resists or "buffers' changes to this pH from the ingredients and/or temperature fluxes. Lastly, divalent cations, usually Mg^{2+}, is included that acts as a cofactor to enhance the enzymatic activity of the Taq-polymerase during amplification by positioning the incoming dNTP appropriately for the correct chemistry to occur.

Stages	Cycle Steps	Temprature	Times	Cycles
1	Initial Denaturation	94 °C	5 minutes	1
2	Denaturation	94 °C	15 seconds	40
2	Annealing	62 °C	45 seconds	40
2	Extension	72 °C	45 seconds	40
3	Final Extension	72 °C	10 minutes	1

Figure 6. **The three stages of PCR**. Each row represents the five PCR steps, and the columns indicate the name of the step, temperature, time and number of cycles, respectively

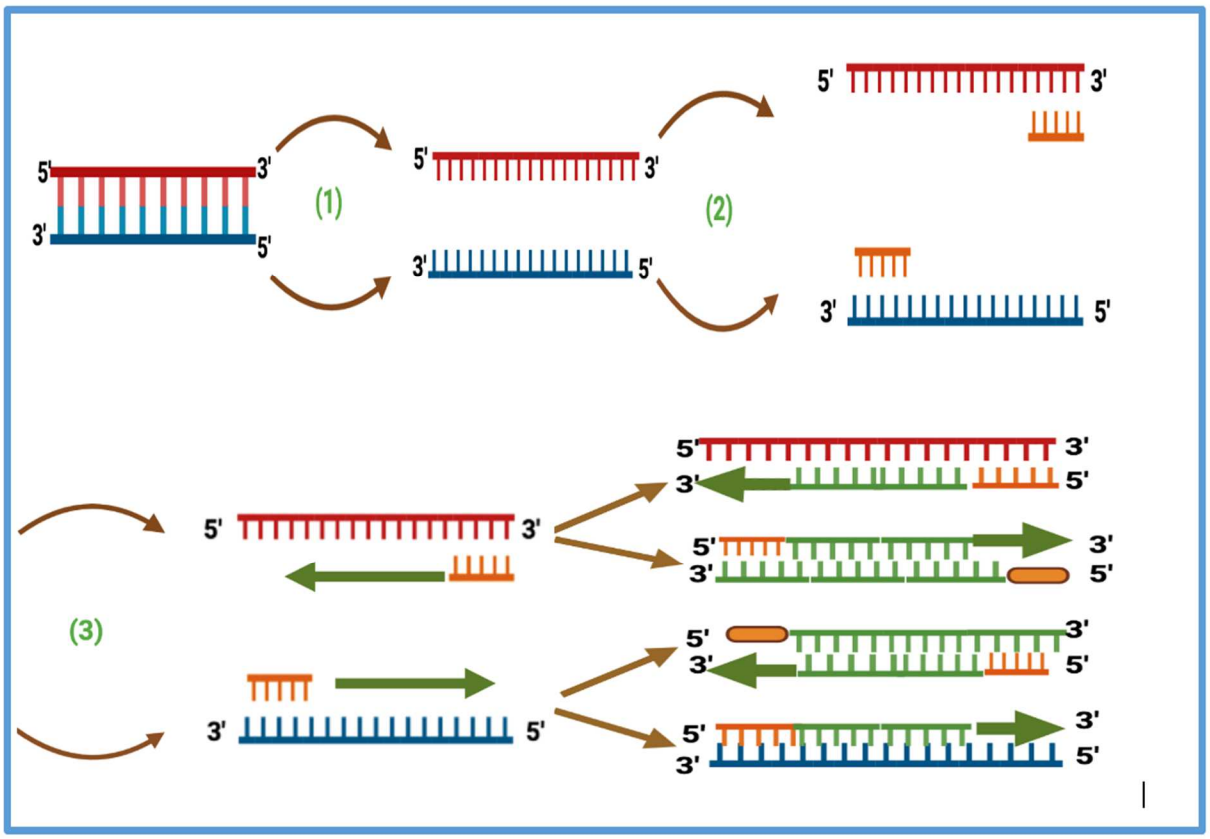

Figure 7. **PCR reaction highlighting the second stage with the three cycles** of (1) denaturation of dsDNA to ssDNA, (2) annealing of oligonucleotides primers to DNA template, (3) extension of DNA amplification by Taq-polymerase.

2.2. Materials and Methods

2.2.1. Mice

WT C57BL/6J mice were commercially purchased from Jackson lab (The Jackson Laboratory, Bar Harbor Maine, United States). VIP heterozygous (HET) breeding pairs were gifted from Professor James Waschek at the University of California, Los Angeles (Colwell et al., 2003). VPAC1 and VPAC2 HET breeding pairs were gifted from professors Sue O' Dorisio (Fabricius, Karacay, et al., 2011) and Anthony Harmar (Harmar, et al., 2002). HET mice were bred at North Dakota State University and all research was approved by the Institutional Animal Care and Use Committee (IACUC) at NDSU. Mice were housed in polycarbonate cages

containing Alpha-Dri paper bedding (Animal Care Systems, Centennial, CO United states). Mice were fed 5001 Lab Diet standard mouse chow (St. Louis, MO, United States) and tap water *ad libitum* with a 12-hour light/dark cycle per day. Breeding cages consisted of one or two female HETs with one male HET mouse and litters were cohoused with parents until weaned at 4 weeks of age. Mice were ear clipped for identification and tail biopsies obtained during weaning.

2.2.2. Mouse Tail Biopsies

Mouse tail biopsies were taken at 4 weeks of age and DNA extracted. The extraction solution (Cat. # E7526, Sigma), tissue Prep (Cat. # T3073, Sigma), and neutralization buffer (Cat. # N3910, Sigma) used for DNA extraction was purchased from Sigma (Missouri, United States). These solutions successfully lysed cells to release DNA that acted as a template for genotyping tail biopsies consisting of clipped (2-4 mm) tissue. Tail samples were placed (dry) into a 1.7 ml centrifuge tube on ice and stored at -20°C until assayed. DNA extraction was performed as described by the manufacturer with modifications. Briefly, 50 µl of extraction/tissue prep master mix was added (40 µl of DNA extraction solution and 10 µl of tissue prep solution per tail sample), centrifuged ≈5 seconds to make sure the entire tail sample was submerged into the master mix, and incubated at room temperature for 20-120 min (typically 20 minutes). Samples were placed at 95°C for 4 minutes followed by the addition of 40 µl neutralization solution to return pH to neutrality, and DNA extracts were vortexed for 30 seconds. Extracted DNA samples (10 ul) were diluted (1/20) in 190 ul of TE buffer (100 mM Tris pH 7.4, 10 mM EDTA pH 8.0) and stored at 4°C until needed for PCR reactions.

2.2.3. PCR

PCR reactions contained 1X GoTaq G2 master mix (Promega, Madison, WI, United States), 312.5 nM of sequence-specific forward and reverse primers, and 2 ul of DNA template

(1/20) dilution in TE buffer or 2 µl nuclease free water. PCR consisted of the following cycling parameters: 94°C$^{(5:00\ min)}$ + [94°C $^{(0:15\ sec)}$ + 62°C $^{(0:45\ sec)}$ + 72°C $^{(0:45\ sec)}$ X 40] + 72°C $^{(1:00)}$. PCR products were separated by 1% agarose gel electrophoresis and visualized by using EZ-Vision dye (Amresco, Radnor, PA, United States). DNA species were visualized by applying UV light (254 nm) and photographed with a digital camera (Alpha Innotech). Table 2 lists all primers used for PCR reactions for the genotyping of mouse strains in the Dorsam Research Group.

Table 2. List of primers used for the indicated mouse strains.

Strain	Primer	Primer Sequence	Reference
VIP	WT Forward	5'-TTTCAAGGTGTGGGGTAGAGACATACA-3'	Colwell CS et al., 2003
	KO Forward	5' - GCCCGGAGATGAGGAAGAGGAGAACAG-3'	
	Common Reverse	5'- TTACCTGATTCGTTTGCCAATGAGTGAC-3'	
VPAC1	WT forward	5'- GGTTGCCATGGCTATCTTGA-3'	Fabricius D et al., 2011
	WT reverse	5 – AGTGGTCTGTCTCCCCGTTGTT-3'	
	KO forward	5'- TTCAACTGTTTTCCCCCATTCAC- 3'	
	KO reverse	5'- CCAGCTCATTCCTCCCACTCA – 3	
VPAC2	WT forward	5'- CGAGAGAGCAGAGCTGACAA-3'	Harmar AJ et al., 2002
	Common revers	5'- TAGGGGTGTTCCCAACTCCA-3'	
	KO forward	5' – GCTTCCTCGTGCTTTACGGT- 3'	

2.2.4. Gel DNA Extraction

PCR products of expected base pair length were removed from agarose gels by a razor blade under UV light and placed into 1.7 ml tubes. Next, 750 µl of agarose dissolving buffer ADB (Cat. # D4001-1-50, Zymo Research) was added to excised gel samples, and incubated at 55^{0}C for 10 min to melt the agarose. Samples were then added onto a Zymo spin column (Cat. # C1003-250, Zymo Research) and placed into a collection tube. Samples were centrifuged for 30 seconds and washed with 200µ l of wash buffer (Cat. # D4003-2-24, Zymo Research) followed by centrifugation for 30 seconds to remove impurities. The zymo-spin column was placed into a new 1.7 ml tube and 10 ul of nuclease free water was added and centrifuged for 1 min to elute

the DNA from the column. DNA yields were measured by using a spectrophotometer (NanoDrop, ThermoFisher, Waltham MA, United State).

2.2.5. Subcloning

The eluted DNA from agarose gels was subcloned into the pCR 2.1 vector by using (Cat. # K202020 Thermo-Fisher) the TA Cloning kit. This kit comes with the subcloning vector, called pCR2.1 (25 ng/ ul), T4 DNA ligase (Units/ul here), and 5X DNA ligase buffer. The procedure was done using a 1:5 ratio of PCR product to pCR 2.1 vector. Our reactions consisted of 10 ng of DNA, 2 ul of 25 ng/ul of vector, 1 ul of T4 DNA ligase, and 2 ul of 5x ligase buffer in a 10 ul ligation reaction volume. Reactions were centrifuged briefly and incubated at room temperature for 15 min, followed by incubation on ice. These subcloned DNA samples were ready for transformation into bacteria.

2.2.6. Transformation

Ligation reactions (2-3 ul) were added into 50 ul of ice-cold competent bacterial cells (M13) and incubated on ice for 30 min. Samples were heat-shocked at 42°C for 45 seconds in a water bath, placed back on ice for 2-3 min, transferred into 250 ul of Super Optimal broth with Catabolites repression (SOC) media and incubated at 37°C shaker for one hour to allow time for transcription and protein translation of antibiotic resistance proteins encoded by the pCR2.1 vector. Transformed bacteria were plated using 100 ul -200 ul of culture and applied by spreading solution evenly onto Luria-Bertani (LB) agar plates containing 100 ul/ml ampicillin antibiotic and 500 ul of 1x X-gal substrate (Thermo Fisher, Massachusetts, United States) to allow for blue/white screening. Plates are incubated by inverting them at 37 °C for 24-48 hr until colonies appeared that were visible. X-gal is a chromogenic substrate that is used for screening the clones containing recombinant DNA. The pCR 2.1 vector has a LacZ gene that encodes B-

galactosidase and links two multiple cloning sites. B-galactosidase cleaves X-gal into 5-bromo-4-chloro-indoxyl, which makes an insoluble blue pigment. If a PCR product is successfully subcloned into the pCR 2.1 vector, the reading frame for the LacZ gene becomes interrupted and any subsequent protein expression results in denatured, inactive protein. As a result of removing B-galactosidase from positively subcloned bacteria, X-gal fails to be metabolized into a blue product and therefore allows for identification of transformed bacteria with a successfully subcloned PCR product ligated in the pCR 2.1 vector. A selection marker was used (Ampliccilin) to identify positively transformed bacteria. The vector, pCR2.1, has both the ampicillin and kanamycin antibiotic genes that render the transformed bacteria resistant to these antibiotics and we used ampicillin as the chosen screening antibiotic. (**See Fig. 8)** for colony screen.

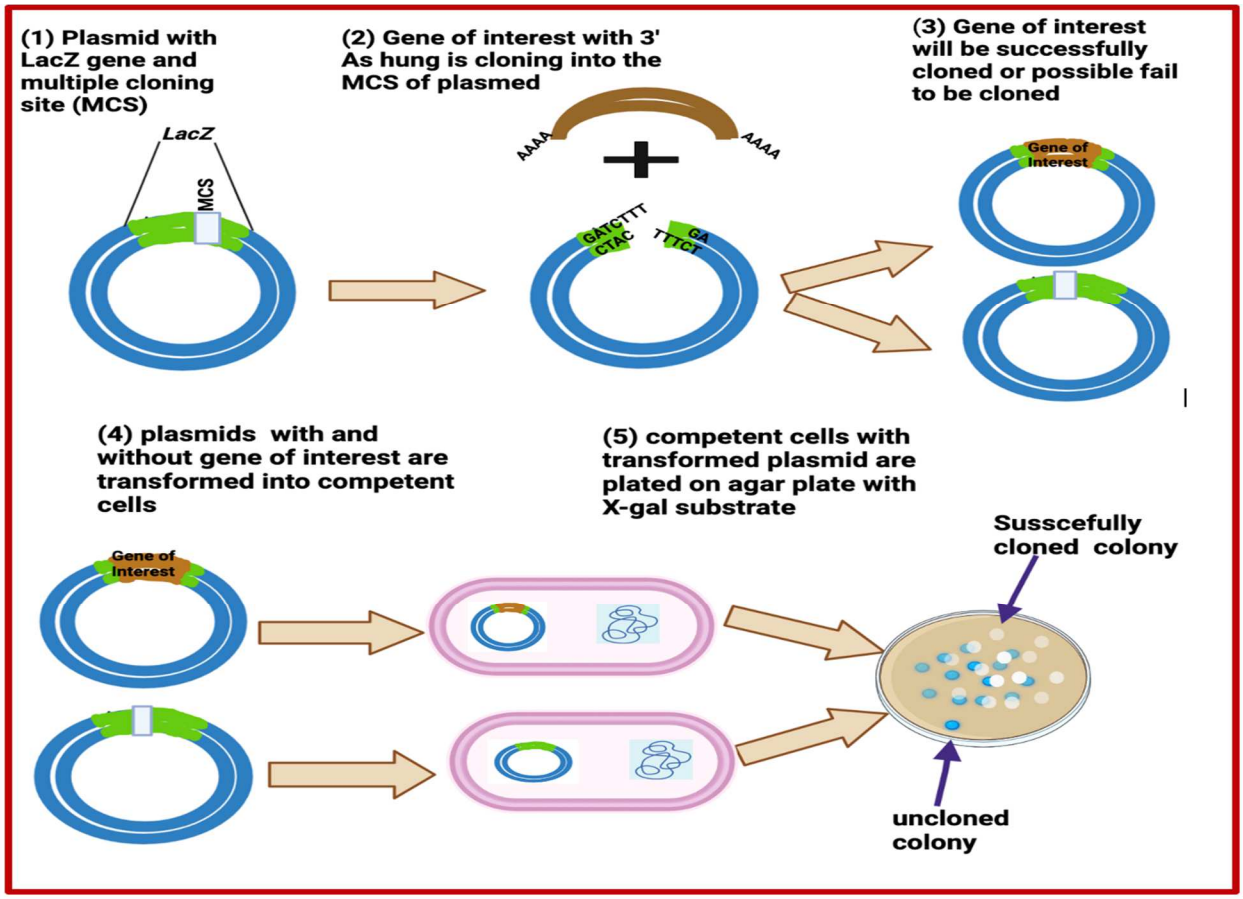

Figure 8. **Construction of vector with LacZ gene. LacZ gene gets disrupted with insertion of the PCR product of interest within the MCS**. After transformation into competent bacteria cells blue/white screening and ampicillin allows for identification of positive bacteria colonies to be cultured and analyzed for the expected PCR product.

2.2.7. Inoculation/Miniprep

A single white colony - which should possess a PCR product - was transferred by a sterile, disposable toothpick from the agar plate to 5 ml of LB media containing 100 mg/ml Ampicillin and cultured on a shaker at 37°C at 300 rpm overnight. The next day, turbid cultures were used to isolate the pCR 2.1 plasmid from bacterial cells by using the Plasmid DNA Mini Kit I (Emego Bio-TEK, Georgia, United State) chromatography technology. Overnight cultures were centrifuged for 1 min at 10,000 x g at room temperature. Supernatants were discarded and 250 ul of solution I was added to pellets, which contained RNase A that destroys contaminating

RNA. Samples were vortexed to mix thoroughly, and suspensions transferred into a new 1.7 mL tube. Next, 250 mL of Solution II was added and gently rotated several times until a clear lysate was seen and incubated at room temperature for another 2-3 min. Solution II contains NaOH that helps to break the cell membrane and disrupts the hydrogen bonding between the DNA bases that coverts dsDNA to ssDNA. Solution III, which has acetic acid and guanidine hydrochloride was then added and immediately inverted several times until a white precipitate formed, followed by centrifugation at maximum speed (> 13,000 X g) for 10 min. A hard white pellet was now visible. The neuralization solution brings the pH down to neutral and the hydrogen bonding between the bases of ssDNA can be re-annealed therefore, ssDNA turns back to dsDNA. It is easy for small circular plasmid DNA to be renatured, but much longer genomic DNA fails to successfully re-anneal in the allotted time. That is why vigorous vertexing must be avoided since it will break the long genomic DNA molecules into small segments that could contaminate the plasmid-prep isolation. The Plasmid DNA is separated easily in the solution and the genomic ssDNA, denatured cellular proteins and other debris interact via hydrophobic interaction to form a white precipitate. The white pellet can easily be separated from plasmid DNA in solution by centrifugation. Clear supernatants were transferred into HIBind DNA Mini Colum and centrifuged at maximum speed for 1 min and filtrate discarded. HBC buffer was added (500 ul) with 100% isopropanol (28% final concentration) and centrifuged at maximum speed for 1 min, followed by discarding the filtrate. Added 700 ul of DNA wash buffer that was diluted with 100% ethanol followed by centrifugation at maximum speed for 30 seconds, again discarded the filtrate and reused the collection tube. Centrifuged the empty HIBind DNA mini column at maximum speed for 2 min to isopropanol from the column. Transferred the HIBind DNA mini column into a clean 1.7 ml tube and added 40 ul of TE buffer followed by incubated

at room temperature for 1 min, centrifuged at maximum speed for 1 min to elute plasmid DNA from column and the eluted DNA was stored at -20°C for future use.

2.2.8. Digestion

To confirm that a PCR product were successfully cloned into the vector, digestion with an endonuclease was employed. The pCR 2.1 vector has an EcoRI restriction site flanking the multiple cloning site and therefore will release the subcloned PCR product that can be visualized for the expected size. Our digestion reaction contained 500 ng of plasmid or miniprep product, 2 ul of 10 X restriction buffer, 2 ul of restriction enzyme (EcoRI) (BioLab, Massachusetts United States), brought up total volume to 40 ul with water. Reactions were centrifuged and briefly mixed to spin down all material and incubated at 37^0C for one hr in a waterbath. Loading dye Blue/Orange (Promegan, Madison, Wisconsin, United States) was added 5 ul of 10 X , followed by a brief vertexing . Digested reactions were subjected to separation on a 1% agarose gel electrophoresis containing EZ-Vision dye for visualization on a UV light (254 nm) and photographed with a digital camera (Alpha Innotech) (**See Fig. 9**)

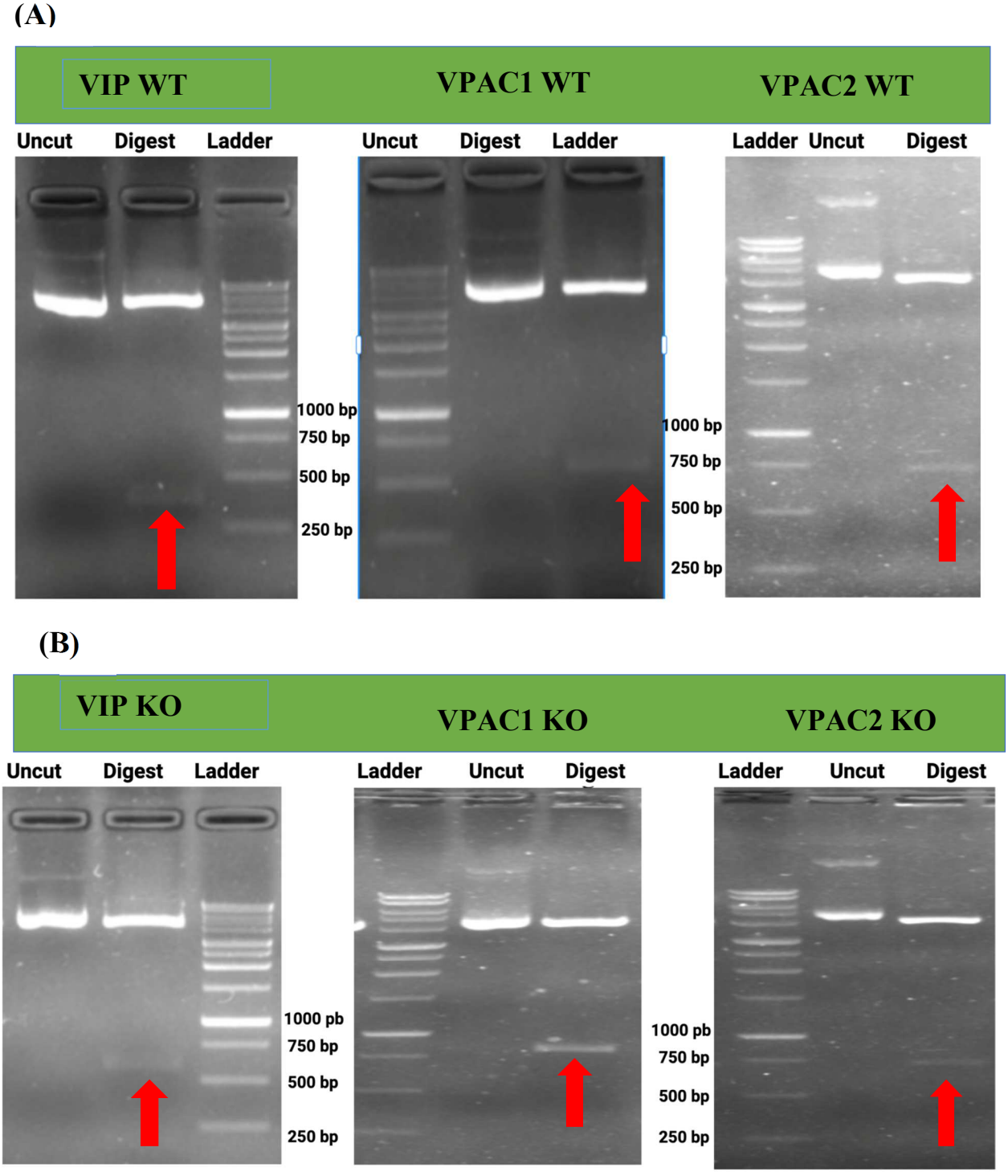

Figure 9. **Digestion results for PCR products as indicated for all three strains** and for A) WT B) KO.

2.2.9. Sequencing

Restriction digestion reactions that generated the expected excised DNA species were selected for sequencing. DNA (100 ng) was sent by FedEx to Sequetech Corporation (Mountain View California,) for sequencing by utilizing (M13 forward and revere primers). Nucleotide sequences obtained from bidirectional sequencing were blasted to the NCBI database to confirm sequence agreement with the expected gen of interest. The pathway to use the NCBI website to BLAST fasta nucleotides are shown in (**fig.10**).

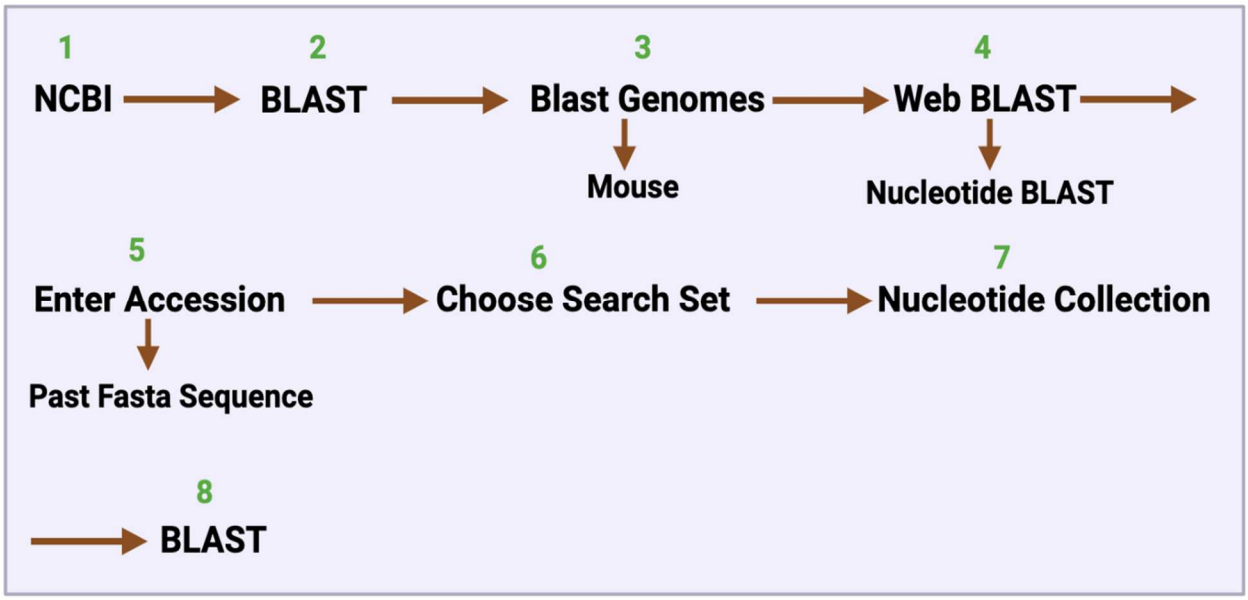

Figure 10. **Sequencing strategy**. This pathway shows the steps needed to BLAST nucleotides by using the NCBI website. Sequence results after BLAST on NCB1 websites are shown in Figure 11.

2.3. Result

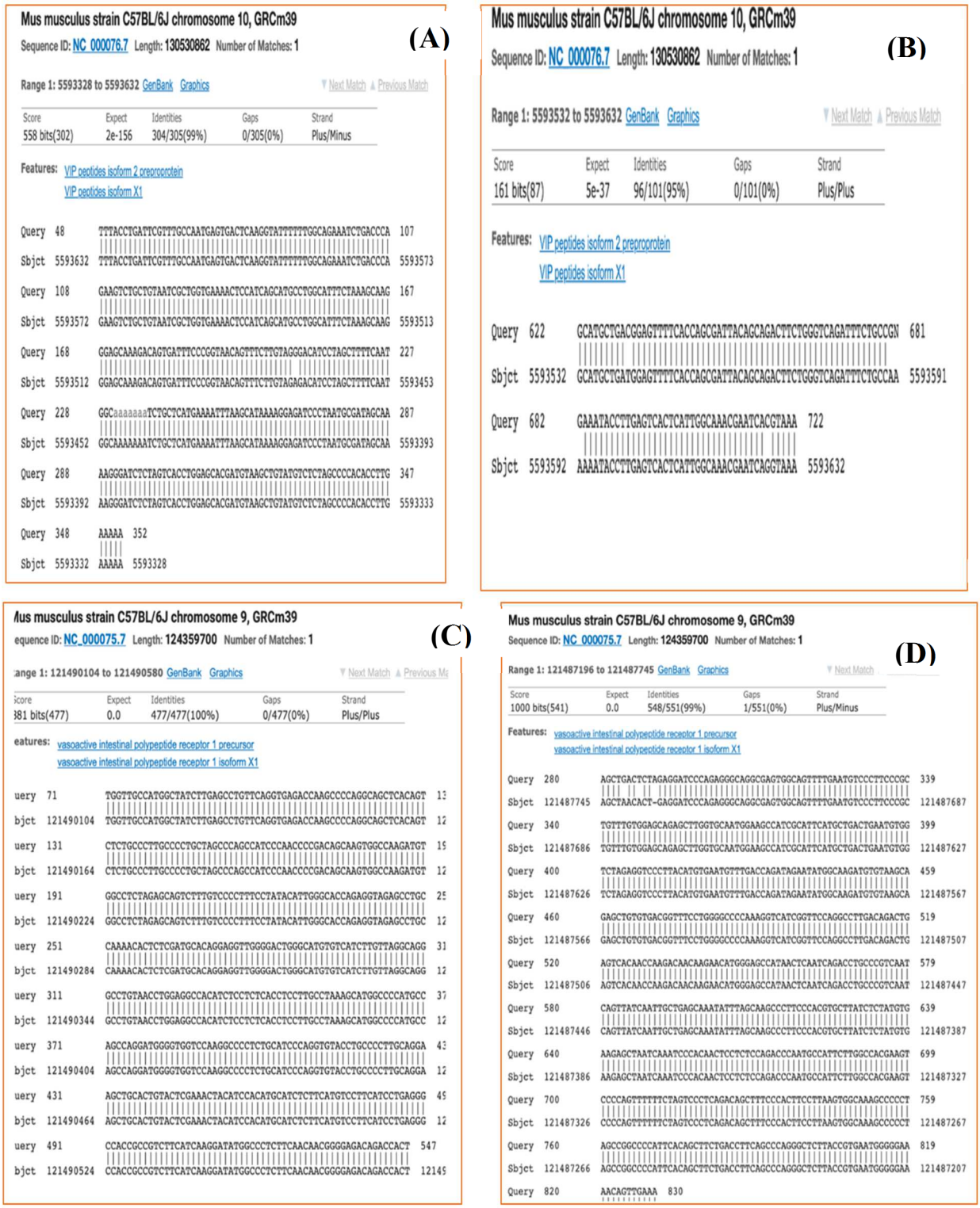

Figure 11. Sequence results by BLAST on NCBI website. A). VIP WT, B) VIP KO, C) VPAC1 WT, D) VPAC1 KO, E) VPAC2 WT, F) VPAC2 KO.

Figure 11. Sequence results by BLAST on NCBI website. (continued) A). VIP WT, B) VIP KO, C) VPAC1 WT, D) VPAC1 KO, E) VPAC2 WT, F) VPAC2 KO

3. ROLE OF VASOACTIVE INTESTINAL PEPTIDE IN PROPIONATE- INDUCED REGULATION OF GLUCONEOGENIC mRNA EXPRESSION

3.1. The Obesity Epidemic

Obesity is a 21st century worldwide epidemic and has become a major socioeconomic health burden. The World Health Organization (WHO) considers a person overweight with a body mass index (BMI), which is the ratio between body weight (kg) and the square of body height (m), over 25 kg/m and obese over 30 kg/m, respectively. Currently, 42% of adults are obese in the United States and this incidence is increasing rapidly. Obesity is a chronic medical disorder involving an excessive amount of fat caused by a net increase in energy entering the body versus energy expenditure. According to the WHO report in 2021, obesity accounted for approximately 2.8 million deaths from comorbidities, including cardiovascular diseases, diabetes, certain cancers, neurological disorders, chronic respiratory diseases, and digestive disorders. The estimated annual medical cost in 2020 for obesity and related comorbidities in the United States was nearly $173 billion dollars, and adults who were obese had $1,861 excess annual medical costs per person in 2019 (Ward et al., 2021). As the obesity rate in America is increasing, the list of diseases associated with obesity is also increasing. Studies found that obesity has been linked with several mental disorders, including anxiety, personality disorder, attention deficit hyperactivity disorder (ADHD) trauma, mood disorders, and schizophrenia (Avila et al., 2015). There is a fatal flaw in our current approaches to successfully treat and safely control human obesity. It is imperative to develop novel medical interventions in addition to diet, exercise, and bariatric surgery – the only surgical procedure currently in place to treat life-threatening obesity - in an attempt to curve the obesity epidemic.

3.2. Maternal Obesity

Maternity obesity plays a key role in the health of the offspring and research shows obesity in mothers can increase the risks for child obesity. It is now well established that the phenotype of an individual is driven by in utero environmental conditions (Chadio S et al., 2014). There is also clearer evidence that maternity obesity significantly impacts cognitive functions and mental health of the offspring and increases the risk of cognitive disabilities and psychiatric disorders such as ADHD, autism, anxiety, depression and eating disorder in the offspring later in life (Buss et al., 2012). Obesity by the mother during pregnancy also results in neuroendocrine, metabolic, and immune changes, which can influence fetal exposure to hormones and inflammatory cytokines. These changes can lead to altered behavioral regulation and reduced working memory performance in early childhood (Cirulli et al., 2020). Generally, the evidence suggests that pre pregnancy obesity is more harmful to the fetus than weight gaining during pregnancy (Cirulli et al., 2020). Overall, obesity is a dangerous epidemic that affects our economy, social, physical, and mental health. Before it is too late, better clinical management of obesity is crucial.

3.3. Gut Microbiota

The GI tract consists of trillions of different microorganisms that play vital roles in host physiology, immunity, and metabolism (Dethlefsen L et al. ,2006). The host shares a symbiotic relationship with their microbiota. A stable GI tract environment is also crucial for gut microbiota homeostasis and contributes to positive metabolic health benefits, including weight glucose, and insulin homeostasis (Neish et al.,2009). Some dietary fibers, such as oligosaccharides, cannot be digested by host enzymes, and therefore must be metabolized by the gut microbiota. Waste products from the digestion of host-nondigestible complex carbohydrates

(e.g., fiber from plants) are called short chain fatty acids (SCFA), butyrate, propionate, and acetate. SCFA are important for host health as they act as an important energy source for intestinal epithelial cells and can also bind host receptors thereby regulating cellular functions (Zhan et a., 2020; De-Vadder et al., 2015). Our lab has reported that vasoactive intestinal peptide (VIP), a neuropeptide delivered to the gut by the enteric nervous system, is a homeostatic regulator of the gut microbiota in female and male mice (Brains et al., 2019). Moreover, our group recently published a follow-up paper demonstrating that VPAC1 was the primary driver for this homeostatic influence of the gut microbiota by VIP (Ericsson A. et al. 2021)

3.4. Intestinal Gluconeogenesis (IGN)

The genes that the gut microbiota encode for are referred to as the microbiome. It is the gut microbiome that encodes for enzymes capable of unlocking additional caloric energy from host-nondigestible fiber. SCFA has been reported to improve metabolic health by regulating glucose homoeostasis, insulin sensitivity, energy expenditure, and lowers body weight (e.g., important for the morbidly obsess). Some studies have linked such positive metabolic outcomes to the induction of intestinal gluconeogenesis (IGN; De Vadder et., 2014, 2015). Evidence for IGN promoting positive health benefits was from studies utilizing six-week-old rats fed a propionate-enriched diet for two weeks that exhibited elevated enzymatic activity levels of the gluconeogenic rate-limiting enzyme, G6Pase, compared to a control chow-diet. (De Vadder et al., 2015). The same author reported one year later that butyrate induces G6Pase (and other IGN genes) directly, but propionate is dependent on a functional enteric nervous system. Their data to support this conclusion was using neurotoxin-treated rats (e.g., capsaicin), butyrate fed mice exhibited increased protein and enzymatic activity of the IGN gene, G6Pase, in jejunum samples, but propionate fed mice failed to show such changes (De Vadder et al., 2016). The authors

concluded that butyrate induced IGN gene expression changes are direct by entering IECs and increasing ATP and cAMP.In contrast, propionate induction of IGN gene expression was dependent on enteric neuronal signaling. Additionally, the authors speculated that the neurotransmitter, VIP, might be acting as a "local mediator" to mediate propionate-induced upregulation of G6Pase expression and enzymatic activity. To test this idea, they compared rats fed propionate for two weeks to rats fed a control diet and demonstrated that: (1) there was elevated immunoreactive VIP levels in jejunum tissue by immunofluorescence, (2) inhibition of G6Pase enzymatic activity by a VPAC1 inhibitor, and (3) elevation of intracellular cAMP and phosphorylated cAMP responsive element binding protein (CREB) bound to the promoter of the G6Pase gene by ELISA and Chromatin immunoprecipitations. However, a major limitation to this study was that the authors conducted their experiments with wildtype animals rather than VIP null animals. Moreover, there data was circumstantial at best showing increased VIP immunoreactive material and VPAC1 signaling involvement with the use of a pharmacological drug in propionate-fed mice. However, these observations are fought with problems. For example, food intake has been shown to increase VIP release from the enteric nervous system and therefore the elevated VIP immunoreactivity might have been from their diet per say and not exclusively from propionate (Talbot et al. 2019). Also, the use of pharmacological inhibitors can have off-target effects, and the secondary messenger, intracellular cAMP, is enhanced by numerous extracellular factors within the gut and not exclusively by VIP (Sutherland et al., 1958). That said, it is enticing to propose that VIP might be linked to propionate-induced upregulation of G6Pase and other IGN gene expression and enzymatic activity to influence the positive metabolic benefits on glucose metabolism for gut microbiota-derived metabolites, like propionate. Therefore, we initiated a similar propionate-enriched mouse chow diet using VIP

deficient mice to test whether VIP is a "locator mediator" (De Vadder et al., 2015) for propionate-induction of gluconeogenic mRNA expression, glucose 6 phosphatase (G6pase), fructose 1,6 biphosphatase (FBP1) phosphoenolpyruvate carboxykinase (PCK1), and pyruvate carboxylase (PCX) by digital PCR (dPCR).

3.5. Gluconeogenesis

Gluconeogenesis is a metabolic process where an organism produces glucose from non-carbohydrate precursors such as propionate, glycerol, and AA. This process occurs mainly in liver and kidney of mammals when blood glucose becomes too low. Glucose is the main source of energy for brain, muscles (in the form of glycogen) and red blood cells, and the steady supply of glucose is crucial for these tissues to maintain normal physiological function. The liver is te primary organ in the maintenance of glucose homeostasis because it regulates blood glucose at a constant level and accounts for about 75% of endogenous glucose production. When the level of blood glucose becomes high in bloodstream, for example after a meal called the postprandial state, excess glucose is taken up by the liver and stored as glycogen via glycogenesis. Under fasting conditions, low carbohydrate diet, or excessive exercise, the liver generates glucose by breaking down glycogen stores via glycogenolysis (Oh KJ et al., 2013). Prolonged starvation causes the depletion of hepatic glycogen stores that in turn induces glucose biosynthesis shunting pyruvate from entering the TCA cycle to become a metabolite for gluconeogenesis. The hormones which control the balance of glucose in the blood are glucagon and insulin. When glucose is high in the blood, insulin is released into the circulation by the beta cells of the pancreas and the ratio between insulin and glucagon becomes high. In contrast, when blood glucose is low, glucagon is released from the alpha cells of the pancreas and the ratio between insulin and glucagon becomes low. Gluconeogenesis substrates are SCFA such as propionate

produced by the gut microbiota, AA such as alanine that becomes elevated in the gluconeogenic state, and glycerol, a metabolite generated from lipolysis. Gluconeogenesis is the reverse process of glycolysis, as glycolysis is a catabolic pathway that converts glucose to pyruvate, while gluconeogenesis is an anabolic process that converts pyruvate to glucose. Both pathways share common and unique enzymes. Glycolysis has 10 enzymatic steps, three of which are irreversible. They are hexokinase, phosphofructosekinase-1, and pyruvate kinase. The net product of glycolysis is two pyruvate molecules, two ATPs, and two NADH + H^+, while the net product of gluconeogenesis is: Glucose + 4 ADP + 2 GDP + 6 P_i + 2 NAD^+. Therefore, gluconeogenesis requires significant amounts of energy for its biosynthesis, but is physiologically necessary when glycogen is depleted and blood glucose levels are low to fuel the brain, red blood cells and regenerate the glycogen stores in muscle. The first step of gluconeogenesis is conversion of mitochondrial pyruvate to oxaloacetate by pyruvate carboxylase, an enzyme activated by high acetyl-CoA levels that occurs during fatty acid oxidation. This step is energy consuming, as it needs two ATP molecules. Mitochondrial oxaloacetate cannot pass through the mitochondrial inner membrane and so it must first be converted to malate by mitochondrial malate dehydrogenase needing 2 NADH + H^+s. Malate can then be shuttled across the mitochondria's inner membrane and into the cytoplasm, where it is subsequently converted back into oxaloacetate by cytoplasmic malate dehydrogenase. The second unique step in gluconeogenesis is catalyzed by PEP carboxykinase (PCK1 is our abbreviation) and converts oxaloacetate to PEP in the cytoplasm requiring two GTP molecules. Conversion of PEP to fructose 1,6, bisphosphate is reversible and are shared with the glycolysis pathway. The third unique step in gluconeogenesis is the conversion of fructose 1-6, bisphosphate by FBP1 to fructose-6-phosphate. Again, conversion of fructose-6-phosphate to glucose-6-phosphate is reversible and

the same enzyme catalyzes this reaction in glycolysis, called phosphohexose isomerase. The fourth and final unique step of gluconeogenesis is the conversion of glucose-6-phosphate to glucose by G6Phase, which is irreversible and differs from glycolysis and takes place in the endoplasmic reticulum (ER) as G6Pase is an integral membrane protein within the ER (**See Fig.12**). G6Pase is also used for the final dephosphorylation of glucose-6-phosphate during glycogen breakdown, but since this is separate from glycolysis, we will consider that G6Pase is a fourth unique enzyme in gluconeogenesis.

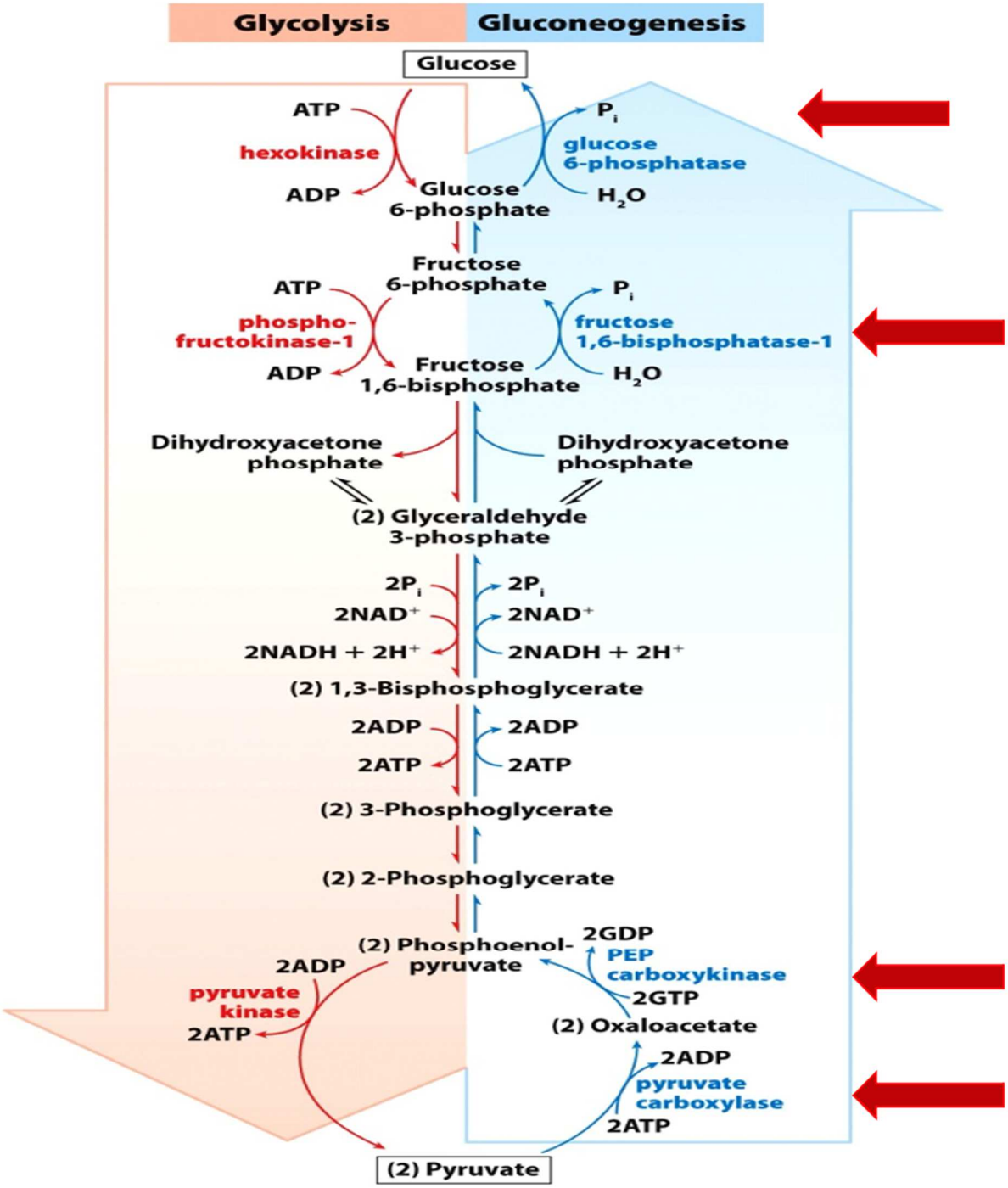

Figure 12. **Glycolysis (left, pink shaded) and gluconeogenesis (right, blue shaded) pathways.** Seven reversible steps are catalyzed by the same enzymes in both pathways while three (glycolysis) or four (gluconeogenesis) unique enzymes catalyzed these pathways. This Diagram is taken from Biochemistry Book (Donald Voet, 12/1/2010).

3.6. Intestinal Gluconeogenesis (IGN)

Two primary functions of the intestines are digestion and nutrient absorption. The intestinal wall is made up of epithelial, immune, nerve and muscle cells. Recently, it was demonstrated that the intestines expressed all four unique gluconeogenic genes most likely in epithelial cells, but the biological relevance was initially unclear as liver, and to a lessor-extent kidney, are responsible for endogenous glucose production (EGP).

The first piece of evidence for intestinal gluconeogenesis (IGN) came from a Swedish group in 1965 that demonstrated intestinal G6Pase expression in human jejunal mucosa. In the same year, another gluconeogenic gene, FBP1, was likewise reported in the lumen of four patients during surgical operations. These early observations of IGN expression in human intestines were focused on the conversion of fructose to glucose in the human jejunum tissue, which highlighted the function of FBP1 (Ockerman et al, .1965). Subsequent observations provided additional pieces of evidence for intestinal gluconeogenesis (IGN). A 1999 report showed that G6pase enzymatic activity (e.g., the rate-limiting step) in the small intestines of rats and humans was readily detected. The authors reported that diabetic rats exhibited 6-8-fold elevated G6Pase mRNA abundance and 300% increase in G6Pase enzymatic activity compared to control rats. These effects were abolished after 10 hrs. post-insulin treatment. This same phenomenon was observed in rat jejunum and duodenum after 48 hours of fasting with mRNA abundance reaching basal levels after 7 hours of re- feeding (Rajas et al., 1999). The same group reported detectable levels of another IGN gene, named PCK1, by Northern blot and enzymatic activity assays. PCK1 mRNA gene expression was higher in the duodenum and jejunum of fasted and diabetic rats (Rajas et al., 2000). These initial results were supported by several additional laboratories in rats and humans.

The production of glucose by gluconeogenic organs (e.g., liver, kidney, and intestines) can vary depending on the nutritional status of the animal. Animals maintained on a standard carbohydrate-based diet results in the liver providing most of the EGP under fed to fasting conditions. After the liver, the kidney is the second most relevant organ providing glucose that contributes a smaller portion of the EGP under a standard diet. Importantly, during prolonged fasting the percentage of EGP by the kidneys increase to compensate and ease the metabolic burden on the liver. In healthy and fed states, the intestines supply only a small fraction (≈ 5%) of the EGP. However, in extreme circumstances, such as during liver transplant procedures and bariatric surgery, the intestines have been demonstrated to contribute to EGP with estimates as high as 30%. Although, there is still debate as to whether IGN truly contributes to endogenous glucose production (EGP) under healthy fed conditions with a standard diet.

Perhaps, the role of IGN is to provide newly synthesized glucose, from SCFA fermentation of fiber for example, to communicate through a gut-brain neural axis that facilitates improved glucose and insulin tolerance by communicating to the brain areas involved in energy homeostasis. In fact, one important outcome for IGN derived glucose released into the portal vein is the capacity to decrease hunger sensation and food intake. Evidence for this has been published documenting that local intestinal treatment with capsaicin, a neurotoxin, prevented the satiety effect. Parallel research showed that diets high in protein also simulated the satiety effect by stimulating a cataplerotic pathway in which AA substrates entered the TCA cycle that in turn activated IGN gene expression to convert these carbon skeletons into glucose via gluconeogenesis. Furthermore, a protein rich diet failed to induce the satiety effect in mice harboring a genetic deletion of the G6Pase gene (Gauteir-Stein et al,. 2021). High-protein diets and high fiber diets can both induce the satiety effect but through compensatory mechanisms;

high protein diets by AA catabolism and high fiber diets by SCFA metabolism that can promote glucose production into the portal vein to influence satiety. Together, both protein and fiber can induce IGN to produce portal glucose that in turn activates the enteric nervous system to stimulate the satiety effect through a glucose sensing mechanism.

In summary, IGN activation by protein rich and high fiber diets are dependent via a not well understood gut brain axis neurotransmitter or neuropeptide mechanism. The metabolic benefits from protein and vegetable diets appears to be mediated by IGN and its final product, glucose, acting as a gut signal to stimulate energy homeostasis in the brain that includes satiety, weight loss and glucose homeostasis. We hypothesize that the gut-brain axis mediator that controls positive metabolic outcomes from protein and fiber diets is vasoactive intestinal peptide.

3.7. Introduction to Digital PCR (dPCR)

Since the last three decades, PCR has played a significant role in molecular biology. The types of PCR are: (1) traditional, end-point PCR, (2) real-time quantitative PCR (qPCR), and (2) digital PCR (dPCR) that is an absolute quantitative option. In 1992, qPCR was founded for the amplification of target nucleic acid by using either fluorescence-based probes or dyes. This technique enables to quantitative detection in real time but is not able to provide absolute quantification of nucleic acids without burdensome standard curves that is time-consuming, expensive, and laborious. qPCR relies on standards and internal references, which require several optimizations (Cao, Cui et.al., 2017). dPCR, on the other hand, is a relatively new technique and is a modified version of tradition PCR, with higher sensitivity better precision. dPCR is very similar to qPCR with respect to the amplification reaction. However, the major difference is that dPCR is an end-base technique that can calculate absolute starting concentrations using the Poisson distribution formula. dPCR reactions are performed based on partitioning a 40 µl

reaction volume into 25,000^{+}, one nL reactions. This portioning strategy allows for the possibility of both positive and negative amplification reactions when the appropriate starting template concentration is used. Positive reactions are determined by an increase in fluorescence signal from a DNA double stranded binding fluorescent dye (e.g., Sybr Green). Negative partitions would generate no fluorescent signal. The term 'digital' indicates the fluorescence presence (e.g., fluorescent or non-fluorescent) in each partition (Witters et al., 2014) that is either fluorescently positive or negative. Quantification is performed by applying the Poisson distribution formula based on the ratio between positive and negative partitions. This absolute detection is highly accurate with p values less than 0.05 for ratios between 4:1 and 1:4 positive to negative partitions, respectively. Outside this range, the accuracy breaks down, and therefore it is imperative to conduct expression curve optimization prior to conducting gene expression experiments. The concept of dPCR was used first by Cetus Corporation in 1988 for detecting β-globin molecules (Saili, Gelfand, et al., 1988). Later, in 1990, this concept was used by Simmonds and Brown to quantify the proviruses in HIV-infected cells (Morley AA, 2014). The term dPCR was coined by Vogelstein and Kinzler in 1999 to measure mixtures of single nucleotide variants by PCR (Vogelstein and Kenzler et al., 1999). However, qPCR was developed and became the gold-standard for laboratories because of it was affordable, precise, high-throughput, and could be used in a multiplexed fashion to analyze multiple gene targets in one bulk reaction. Currently, qPCR is the most popular PCR technique used in molecular biology for the detection and amplification of nucleic acid. However, with recent advancements in microfluidic technology has enabled the development of instruments that can make the sufficient number of partitions consisting of small volume formats (1 nL). Today, dPCR has attracted numbers of researchers and several commercial companies (**See Fig. 13**).

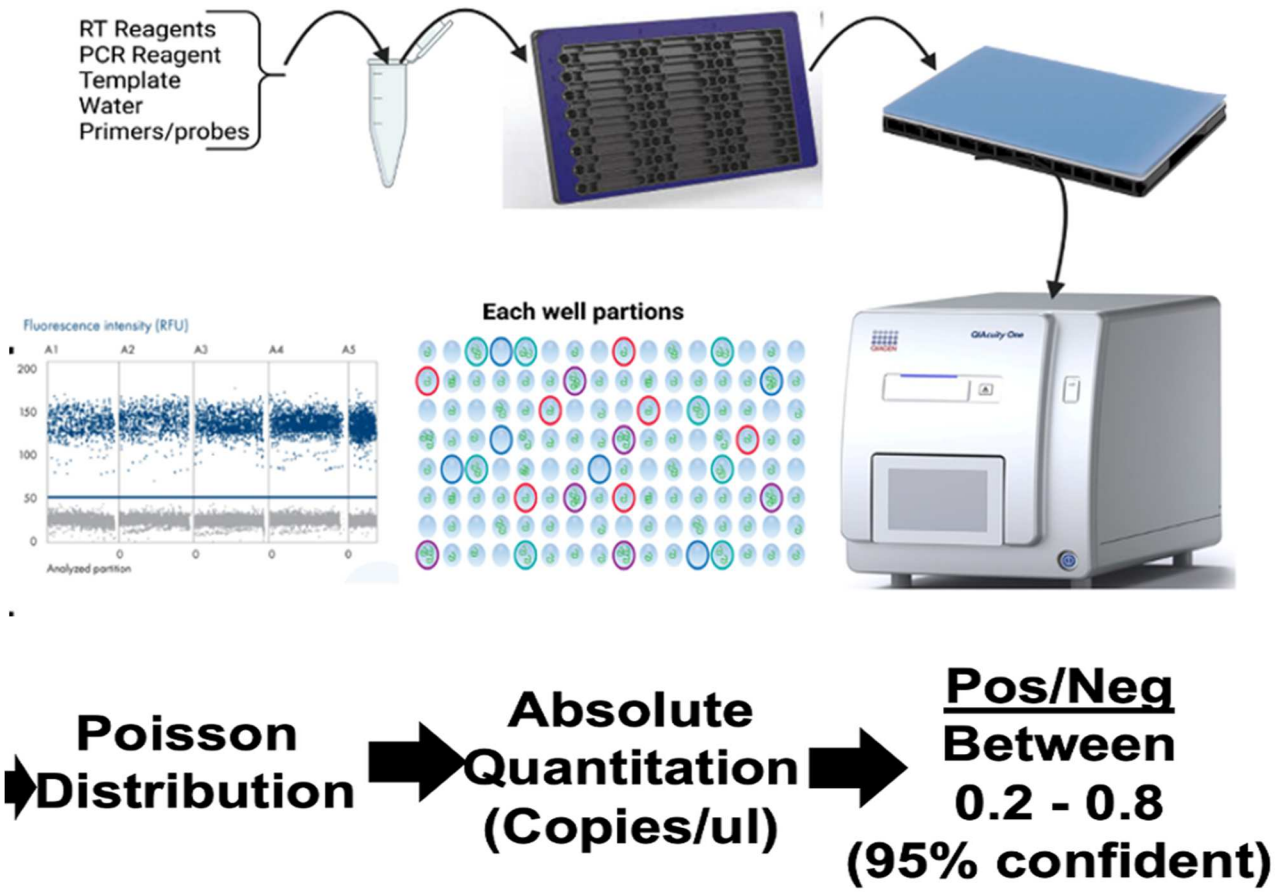

Figure 13**. Workflow for dPCR**. PCR reagents were added to each well (40 ul) and partitioned into 26,000, one nl reaction volumes. Synthesis of first-strand cDNA was initially performed, followed by 40 PCR amplification cycles. A single end-point image was taken by the dPCR instrument. This information was analyzed by the instrument to calculate the ratio of positive and negative partitions. The Poisson distribution formula was then used to calculate the absolute quantitation of starting templets as copies/ul based on the ratios of positive to negative partitions.

3.8. Material and Methods

3.8.1. Tissue Collection

All mouse work was approved by the Institutional Animal Care and Use Committee at North Dakota State University under protocols (A20058 and A 20084). The VIP KO strain (males and females) on a C57BL/6J genetic background (6 weeks old) were randomly separated into two groups and fed either a 100% normal chow 5001 diet (Control) or a 5% (W/W) propionate/95% 5001 diet (propionate-enriched) for two weeks. At 8 weeks of age, mice were

fasted for 3 hours and euthanized with carbon dioxide asphyxiation followed by cervical dislocation as described by the American Veterinary Society Guidelines (2020). Jejunum and liver tissues were harvested by standard organ removal techniques with the middle 6 centimeters of the jejunum segmented into 6 equal, 1 cm samples, while liver tissue was sliced into 1 cm cubes. All tissue samples were frozen immediately on dry ice and stored at -80^{0}C freezer until assayed. Five biological samples were collected from female and male WT, HET and KO mice on standard and propionate-enriched diets (**Table 3**).

Table 3. Tissue sample summary that was used for this study

	Standard Diet (100% 5001)		**Standard Diet (95% 5001) + 5% Propionate**	
	Male	Female	Male	Female
WT	5	5	5	5
Het	5	5	5	5
KO	5	5	5	5
Total	15	15	15	15

3.8.1.1 RNA Extraction

RNeasy Mini Kit (Cat # 74104, Qiagen) chromatography technology was used for RNA extraction as described by the manufacturer. A modified protocol was used for RNA extraction consisting of 3 steps: tissue homogenization, column extraction, and RNA precipitation.

3.8.1.2. Tissue Homogenization

Less than 30 mg of frozen tissue were used for RNA extraction. Tissues were washed with 1 mL of cold phosphate buffered saline buffer (PBS) pH 8.0 by triturating multiple times to remove blood and fecal material. PBS was decanted carefully not to lose the tissue sample. Next, 600 ml of lysis buffer, supplemented with 1.0% β-mercaptoethanol (β-ME), which reduces

disulfide bonds, was added to samples along with a 50 mm stainless steel bead. Samples were placed into a tissue homogenizer (Bead Bug, Microtube Homogenizer Model#: D1030, Benchmark Scientific, Massachusetts United States) for 1 min or until tissues were uniformly homogeneous. Lysates were centrifuged for 3 min at ≥8000 x g. Supernatants were carefully transferred the into a gDNA eliminator spin column and centrifuged for 30s at ≥8000 x g. The eliminator spin column excludes genomic DNA thus allowing for a purer RNA yield. This also negated the need to use DNase. One volume of 70% ethanol was added to the eluant and mixed immediately by pipetting to dissolve away salts from the RNA pellet.

3.8.1.3. Column Extraction

Samples (700 ul) were loaded onto the RNeasy spin column, and placed in a 2 mL collection tube and centrifuged for 30s at ≥8000 x g. The eluant was discarded and the collection tube reused. Columns were treated by three successive wash steps, centrifuged and eluants discarded as described above. The three wash steps were 700 µl of RW1 wash buffer, and two500 ul RPE wash buffer steps added to the RNeasy spin columns. Prior to elution of total RNA, spin columns were centrifuged as above for 1 min to remove residual ethanol. Columns were transferred to a clean 1.7 mL collection tube and 40 ul RNase-Free water added directly to the top of the spin column membrane and incubated for 1 min. Columns were centrifuged for 1 min at 10,000 rpm to elute total RNA from the column. Concentrations and 260/280 purity ratios were conducted by spectroscopy (Nanodrop, ThermoFisher, Waltham MA, United State).

3.8.2. RNA Precipitation

To further improve RNA purity, samples were precipitated with 10 volumes of 100% cold ethanol and frozen at -80°C for ≥ 1hr. To this end, 400 ul of 100% ice-cold ethanol, 15 ul of 3M sodium acetate (pH5.2, 0.3 volume) and 2 ul of 5 ug/ul of glycogen blue were added. Using

sodium acetate provides positive sodium ions that can specifically neutralize the negative charges of the phosphate backbone of RNA, while the ethanol removes the hydration shell of water molecules around the phosphates of RNA because ethanol has a lower dielectric constant than water thus allowing for greater sodium-phosphate interactions. Both effects induce RNA to "let go" of the water/ethanol solvent and precipitate out of solution. Glycogen Blue is stained polysaccharide that also precipitates in the presence of ethanol and is used as a carrier that promotes more RNA to precipitate by "trapping the RNA" as it falls out of solution and allows for a more visible pellet due to the blue stain. RNA samples were centrifuged at high maximum rcf (name of centrifuge) for 20 min at 4°C and supernatants decanted (a blue pellet was visible on the bottom of tube at this stage). A 70% of ethanol wash (500 ul) followed to solubilize salts from the RNA pellet and vortexed for 5 seconds on medium followed by inversion three times and centrifuged as above. Samples were decanted and tubes inverted onto a clean kim wipe to air dry for 5 min. RNA was reconstituted using 40 ul of TE buffer and concentrations were determined by spectroscopy at 260 nm wavelength (NanoDrop, ThermoFisher, Waltham MA, United State).

3.8.3. Measuring RNA Integrity (IQ)

To estimate the percentage of full-length, intact mRNA species (RNA integrity), RNA samples were evaluated prior to moving onto dPCR. For reproducibility, only RNA that resulted in IQ ratios of 6.5 or higher were assayed. The Qubit RNA IQ Assay Kits (Cat #: Q 33221, ThermoFisher, Eugene Oregon, United States) measured RNA integrity using a fluorescence-based assay as described by the manufacturer. Briefly, two different fluorescent dyes were added to a diluted sample of total RNA (50-150 ng/ul), where the first dye binds highly structured, intact RNA and the second dye selectively binds small, degraded RNA. The instrument

calculates the ratio between both dyes and gives an "IQ score" between 1-10, with a "10" being full-length, intact RNA and a "1" being fully degraded RNA. For example, an IQ of 7 means the sample has 70% highly structured, intact RNA and 30% small RNA. This procedure required making a master mix using 199 ul of IQ buffer and 1 ul of IQ fluorescent dyes per sample, along with 3 standards for instrument calibration and 20% extra for pipetting error. To fresh IQ tubes (Cat#: Q32856, ThermoFisher), 190 ul of master mix and 10 ul of standard or diluted total RNA samples were aliquoted per tube. Samples were inserted into a Quit 4 fluorometer (Cat #: Q33238, Thermofisher) to determine their respective IQ scores.

3.8.4. dPCR

This technique utilized the 24-well, 26k nanoplate dPCR plates (Nanoplate 26k- 24 well QIAcuity Hilden Germany). Each 24-well received 40 ul of PCR reaction mix prepared on ice. This reaction mix contained 4 ul of total RNA at 31.25ng/ul, 10 ul of 4x One-Step RT-PCR master mix, 0.4 ul of 100x multiple RT Mix, 1.6 ul of each primer and probes mix brought the total volume to 40 ul with double distilled (dd) water. Plates were covered with a robber lid and placed into the instrument (QIAcuity Four, Maryland, United States).

Table 4. List of indicated parameters for dPCR

Component	Volume/ Reaction	Final Concentration
4x One-Step RT-PCR MM	10 ul	1 X
100x Multiples RT Mix	0.4 ul	1 X
Primer + probe Mix each	1.6 ul	0.4uM F/R, 0.2uM probe
Water	As needed	
RNA	4 ul	31.25 ng/ul

Table 5. List of primers and probes of four gluconeogenic genes for dPCR

Gene	Name	Sequence
G6pase	Forward	5'-TCC CAA CCA CAA GAT GAC G-3'
G6Pase	Reverse	5'-GCG CAG CAG GTG TAT ACT ATG-3'
G6Pase	Probe	/56-ROXN/AGCCAACGTATGGATTCCGGTGT/3IAbRQSp/
FBP1	Forward	5'-GTA TGC GCT CTA-TGG-CAG-TG-3'
FBP1	Reverse	5'-GTC CAC CAT AAT GAA TTC TCC AAT G -3'
FBP1	Probe	/5FAM/TCCAGCATG/ZEN/AAGCAGTTGACACCA/3IABkFQ/
PCX	Forward	5'-TCA CCA GTG-ACT CTG TCA AAC-3'
PCX	Reverse	5'-ATT GAC CTC GAT GAA GTA GTG C-3'
PCX	Probe	/5Cy5/CCAAGCAGGTAGGCTATGAGAACGC/3IAbRQSp/
PCK1	Forward	5'-ATTGACCTCGATGAAGTAGTGC-3'
PCK1	Reverse	5'-TCACCAGTGACTCTGTCAAAC-3'
PCK1	Probe	/5HEX/TGCCTCTCT/ZEN/CCACACCATTGCA/3IABkFQ/

3.8.4.1. Optimization of dPCR

Since dPCR is absolutely quantification and very sensitive to very small abundant of target template, optimizing of dPCR is essential and it is required to make sure the system runs properly, the primers are sensitive to the target template, and to know the reagents efficiency. Therefore, we diluted our template in one to two dilution and ran dPCR to see how the signal intensity increases with doubling the amount of template (**See Fig.14**). The predicting and the actual sample copies/ul are almost similar and this validation provided data that is required to justify the continued use of the dPCR for analyzing our research project samples.

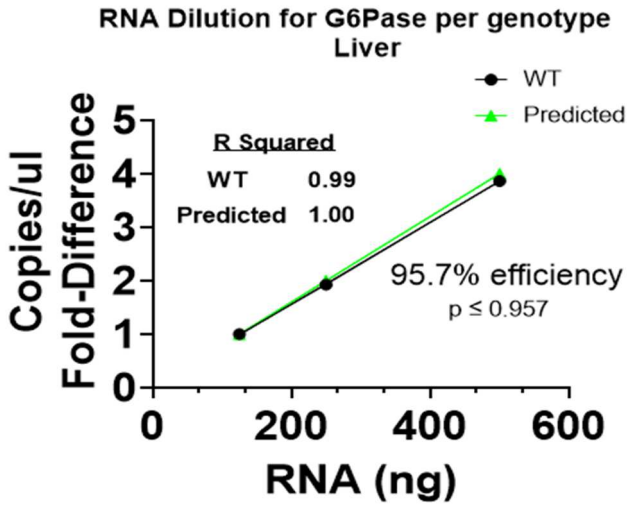

Figure 14. **RNA dilution for dPCR optimization**. The y-axis is the copies/ul and the x-axis is the RNA dilution in ng. The green line is presenting the predicted copies/ul and the black line is presenting the actual sample copies/ul.

3.8.4.2.. Internal Control for dPCR

dPCR is absolute quantitative and it doesn't need reference and standard. However, we used internal control to make sure the system runs properly, how the reagents are stable for a period, technical operation is productive day to day, and so on. For internal control, we used three mice male jejunum samples (VIP WT, VIP HET, and VIP KO) at 125 ng/reaction. Each reaction was multiplexes with three primers (G6pase, FBP1 and PCX) (**See Fig.15**), the internal control for five different dPCR runs.

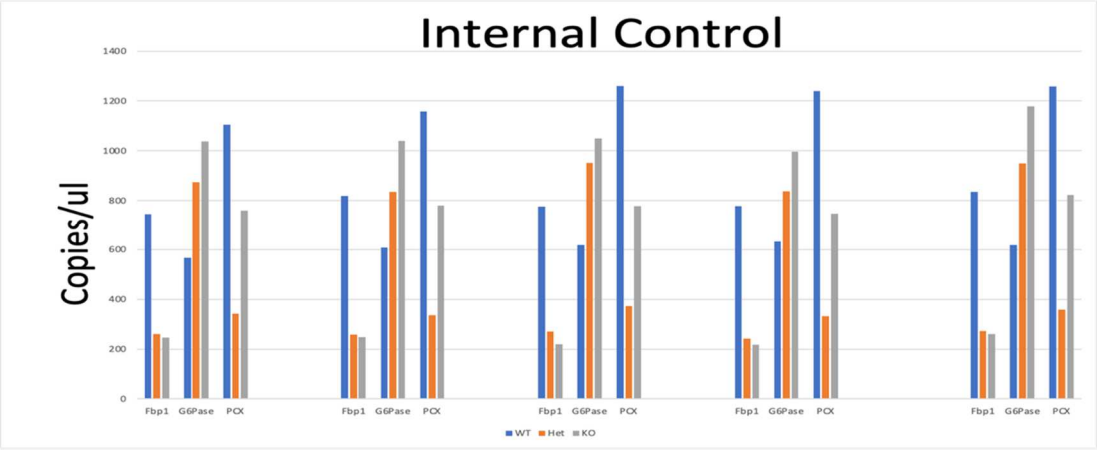

Figure 15. **dPCR internal control**. Y-axis is the copies/ul and the X-axis are five plates run with three primers (FBP1, G6pase, and PCX).

3.9. Result

3.9.1 Are IGN Genes Detectable from Jejunum Tissue at the mRNA Level in Mice Fed a Standard Chow Diet?

It is well-established that the liver and kidney are gluconeogenic organs that supply whole-body glucose production to maintain blood glucose levels at ≈ 1 g/l (Gautier-Stein A. et al. 2021). Such a stable blood glucose concentration is important as glucose is the primary fuel source for brain and red blood cells. Recently, the intestines have been reported to express IGN gene expression (Rajas et al., 1999), suggesting that this organ might be a third gluconeogenic tissue contributing to blood glucose levels. Therefore, our first objective was to recapitulate these observations using WT littermates from our VIP deficient mouse strain and measuring all four gluconeogenic genes by dPCR. To this end, total RNA isolated from male (n=5) and female (n=5) jejunum tissues of mice fed a standard chow diet were used to measure gene expression by a one-step dPCR strategy. Consistent with other research groups, our data exhibited readily detectable mRNA levels (copies/ul) with a similar profile between sexes (**Fig. 16**). The order of gene expression was PCK1>>G6Pase and PCX > FBP1. PCK1 mRNA expression was the highest of all IGN genes (7-15-fold greater) and was statistically significant compared to the other three IGN genes in both sexes ($p \leq 0.05$). Although FBP1 reached statistical significance to PCX in male mice (**Fig. 16A**), it did not reach statistical significance in female mice (**Fig. 16B**). These data confirm IGN mRNA gene expression in jejunum of male and female mice fed a standard chow diet.

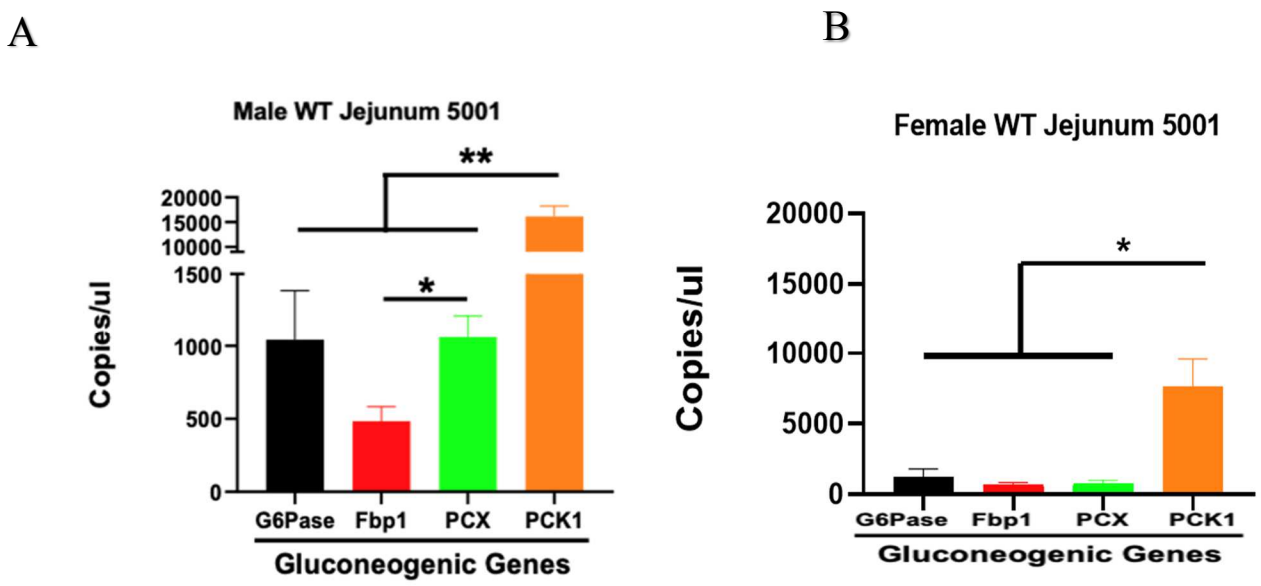

Figure 16. **Basal mRNA levels of IGN genes in mice fed a standard chow diet.** Absolute starting RNA template concentrations (Y-axis) are presented in bar graph form as means +/- SEM (n=5) for the indicated genes in (A) male and (B) female mice. One-Way, unpaired ANOVA analysis with a Turkey multiple comparison test was used to calculate adjusted P values. Statistical significance of $P \leq 0.05$ (*) and $P \leq 0.001$ (**) were considered significant.

3.9.2. Does VIP Signaling Play a Role in Basal Jejunum IGN mRNA Expression Levels in Mice Fed a Standard Chow Diet?

VIP is delivered to the GI tract through the enteric nervous system and is delivered to all layers of the intestinal wall. In fact, approximately half of all enteric nerves are positive for VIP immunoreactivity (Lelievre et al., 2007). We previously published that VIP and VPAC1 deficient mice have substantially altered gut microbiota structures, with both exhibiting elevated Gram-negative phyla (*Bacteroidetes* and *Proteobacteria*) and a depleted Gram-positive Phylum (*Firmicutes*) with reduced bacterial diversity. More than fifty years of research has established VIP as an important GI tract regulator of homeostasis, including digestive enzyme secretion (Nyberg et al., 1992), ion homeostasis, relaxation phase of peristalsis (Lelievre et al., 2007), mucus secretion (Lelievre et al., 2007; Lu et al., 2016), mucus immunity (Nussbaum et a., 2013), intestinal epithelial cell homeostasis (e.g., Goblet cells), and barrier integrity (Wu et al., 2015) .Based on this suite of important modes of action within the intestine, we hypothesized that VIP

signaling through VPAC1, which is exclusively expressed in jejunum IECs, regulates IGN mRNA expression. To test this hypothesis, we repeated dPCR as described above in figure 13. Our analysis revealed significant changes between mRNA levels of 3 of the 4 genes, and a sex-specific difference for PCK1 (**Fig. 17**). In males, PCK1 mRNA levels plummeted by ≈67% ($p \leq 0.05$) in both HET and KO samples compared to WT littermates (**Fig. 17A**). In stark contrast, female PCK1 mRNA levels increased dependent on genotype with KO mice reaching statistical significance ($p \leq 0.05$; **Fig. 17A**). The lowest expressed IGN gene, FBP1, showed consistent decline in mRNA levels in both sexes dependent on genotype, but KO samples did not reach statistical significance in males (males $p \leq 0.2$; females $p \leq 0.05$). G6Pase WT and KO mRNA levels were not significantly altered, but there was an intriguing sex-specific effect in HET samples, with mRNA levels increasing in males but decreasing in females, albeit not reaching statistical significance. PCX expression was not significantly altered by sex or genotype. In total, these data indicate that VIP signaling acts as a positive regulator for FBP1 at the mRNA level in both sexes and PCK1 in males, while VIP signaling is a negative regulator for PCK1 mRNA levels in females.

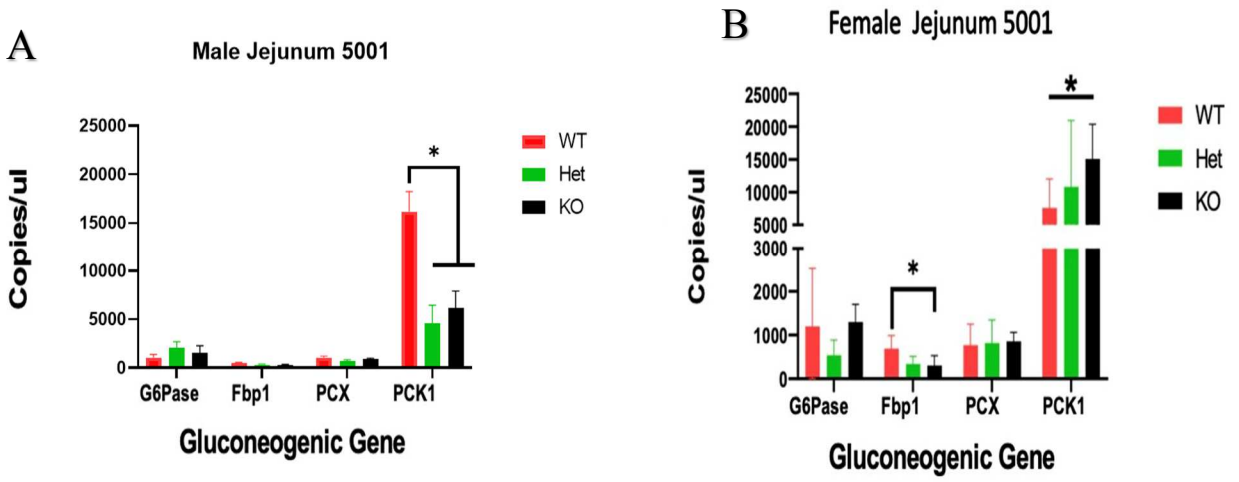

Figure 17. **VIP signaling regulates IGN basal gene expression.** Absolute starting RNA template concentrations (Y-axis) are presented in bar graph form as means +/- SEM (n=5) for the indicated genes and genotypes in (A) male and (B) female mice. One-Way, unpaired ANOVA analysis with a Turkey multiple comparison test was used to calculate adjusted P values. Statistical significance of $P \leq 0.05$ (*) .

3.9.3. Does the Gut Microbiota Metabolite, Propionate, Stimulate Jejunum IGN Expression?

About eight years ago, Professor Gilles Mithieux and colleges published a series of papers showing evidence that short chain fatty acids, derived from fermentation by the gut microbiota, induced IGN gene expression and *de novo* glucose production in fed mice (De Vadder et al., 2014,2015). These reports showed that butyrate and propionate induced IGN expression and glucose production by two different mechanisms. Butyrate regulated IGN directly through a cAMP-dependent pathway most likely due to an increase in ATP as this SCFA was utilized as an energy source. In contrast, propionate induced IGN by a capsaicin-sensitive mechanism indicating a neuronal-dependent mechanism. However, these studies were conducted in rats and therefore we set out to again recapitulate whether propionate (the SCFA focus of my thesis) increased the mRNA levels of IGN genes in WT mice as they did in rats. We employed dPCR as described in Figure 11. Surprisingly, data from this study demonstrated that propionate

did not statistically alter the mRNA expression levels for any IGN gene (**Fig. 18**). Curiously, PCK1 did show a 40-50% decrease in mRNA levels in both sexes but due to the high error between biological samples, it was not statistically significant and will require additional replicates for confirmation. We conclude that propionate does not have a significant effect on IGN mRNA expression and is inconsistent to the data findings in rats. A possible explanation could be that in mice, unlike rats, this regulation is at the protein level and future studies are required to expand on this research front.

3.9.4. A Sex Specific, Haploinsufficiency Mechanism Regulating Intestinal G6Pase in VIP Heterozygous Mice.

De Vadder et al. reported in 2015 that VIP might act as a local mediator to drive propionate-induced IGN gene expression and glucose production by intestinal epithelial cells. However, based on our WT data above that showed little to no alteration in IGN expression from a 2-week propionate diet, we asked the question whether there might be a link between VIP signaling and propionate with respect to IGN mRNA expression. We tested this notion by conducting dPCR as previously described for Figure 13. There was little difference between mRNA levels for all IGN genes in VIP KO jejunum samples in both sexes. However, in heterozygous mice, we again saw a sex-specific difference in G6Pase expression due to a propionate diet (**Fig. 18**). In mice fed a propionate diet, G6Pase mRNA levels decreased in males, and increased in females ($p \leq 0.05$), suggesting that haplo-insufficiency of VIP protein may be a factor in the sensitivity for propionate induction of G6Pase mRNA expression and the potential for glucose production from the intestines.

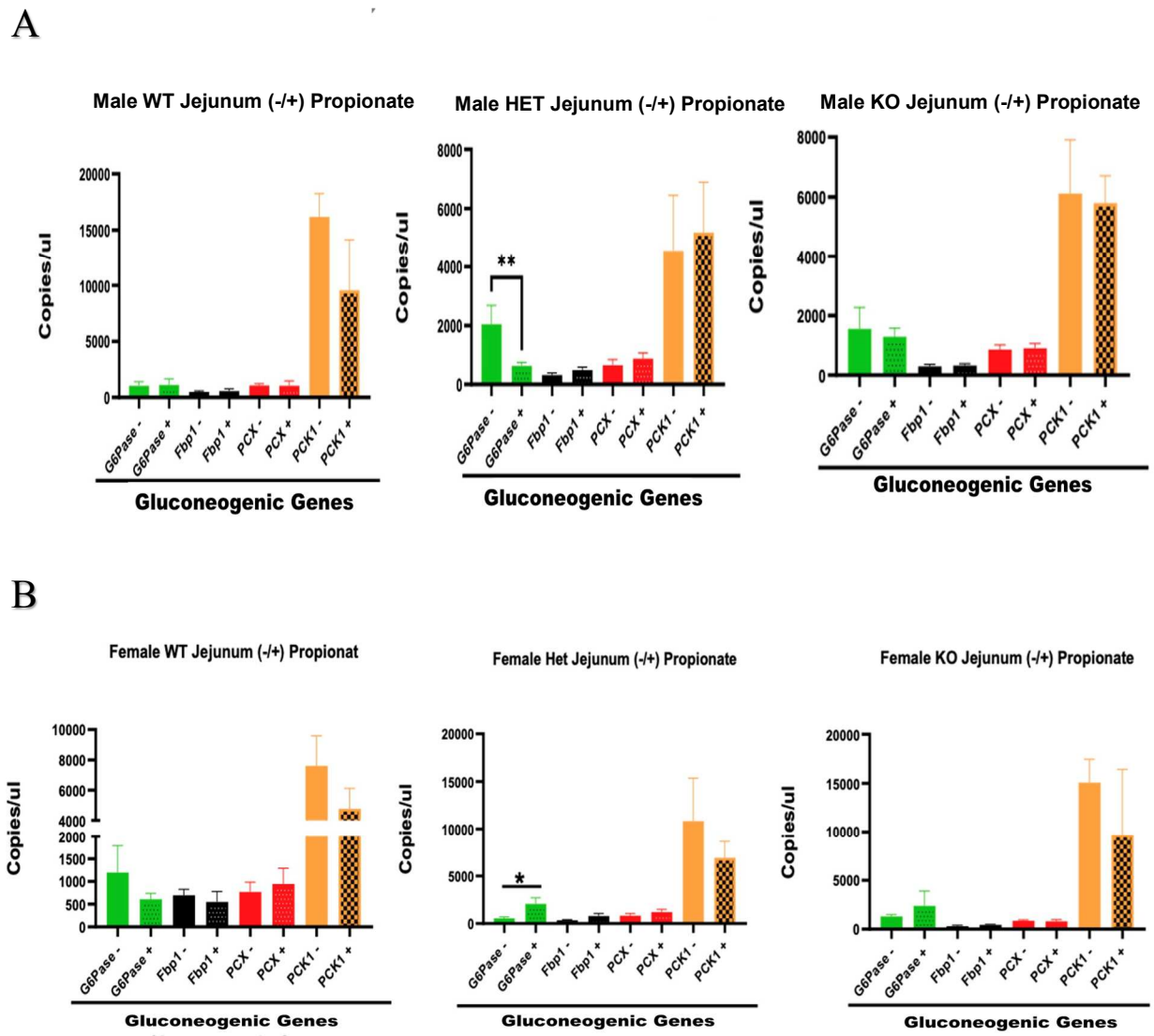

Figure 18. **VIP haploinsufficiency dysregulates G6Pase mRNA expression by propionate.** Absolute starting RNA template concentrations (Y-axis) are presented in bar graph form as means +/- SEM (n=5) for the indicated genes and genotypes in (A) male and (B) female mice. One-Way, unpaired ANOVA analysis with a Turkey multiple comparison test was used to calculate adjusted P values. Statistical significance of $P \leq 0.05$ (*) and $P \leq 0.001$ (**) were considered significant.

3.9.5. Gluconeogenic mRNA Gene Expression is Higher in Liver Versus Intestine.

Gluconeogenic genes from VIP WT mice livers have the same mRNA expression profiles in both sexes, but the expression level is higher in female than male, the opposite trend we observe in intestine (**Fig. 19**). Our results showed that these genes are expressed at higher levels

in liver versus intestine. This finding was expected as the liver is the main gluconeogenic organ in the body accounting for about 75% EGP. G6Pase and PCX had the lowest mRNA expression in both sexes, whileFBP1 and PCK1 were expressed higher in both sexes. PCK1 had the highest mRNA levels compared to the other three gluconeogenic genes in both jejunum and liver.

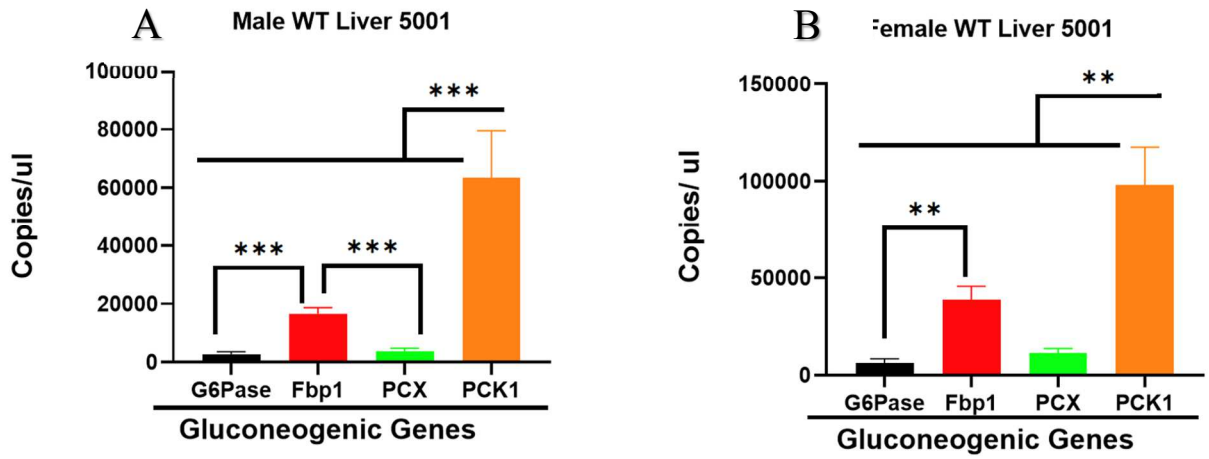

Figure 19. **Gluconeogenic mRNA levels in liver from VIP WT mice fed a standard diet**. Absolute starting RNA template concentrations (Y-axis) are presented in bar graph form as means +/- SEM (n=5) for the indicated genes and genotypes in (A) male and (B) female mice. One-Way, unpaired ANOVA analysis with a Turkey multiple comparison test was used to calculate adjusted P values. Statistical significance of $P \leq 0.001$ (**) and $P \leq 0.0001$ (***) were considered significant.

3.9.6.VIP Signaling Positively Regulates Hepatic GN mRNA Levels in Female Mice.

Our data exhibited that VIP plays an important role in expression of gluconeogenic genes in mouse liver, that reaches statistical significance in females, but not males (**Fig.20**). In female mice, FBP1, PCX and PCK1 were reduced in VIP HET and/or KO mice ($p \leq 0.05$), while G6Pase was downregulated in VIP HET mice but did not reach statistical significance. Noteworthy, is that this decrease in G6Pase from female HET liver tissue was similar to that seen in female HET intestinal tissue. Male mice showed a reduction in PCK1 and an increase in G6Pase HET liver samples, similar to its change in intestinal tissue, but did not reach statistical significance. Taken together, as we observed in intestine, VIP signaling in instrumental at bolstering the

mRNA expression levels of the liver gluconeogenic genes and suggests its involvement in whole body glucose production.

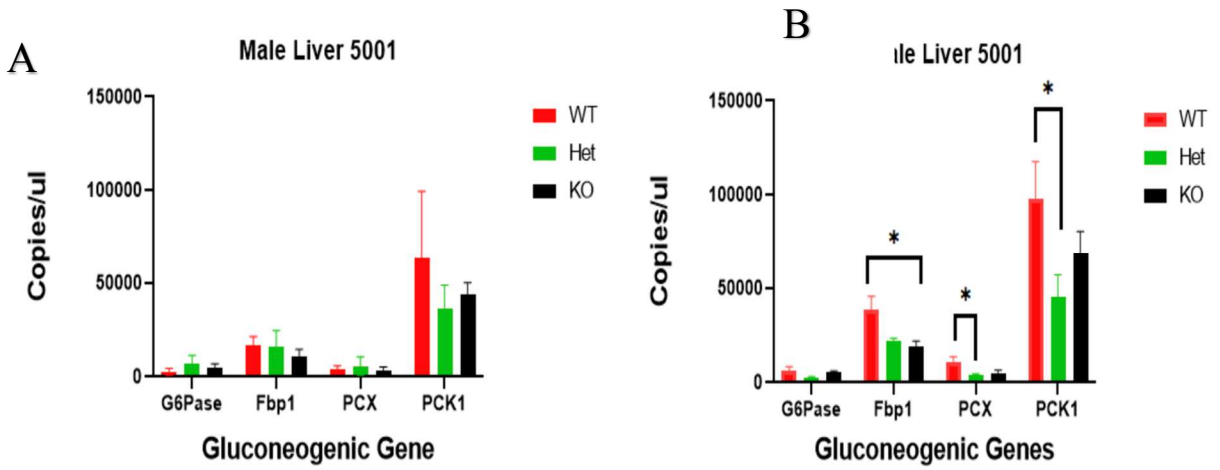

Figure 20. **VIP is a positive regulator for hepatic GN mRNA expression**. Absolute starting RNA template concentrations (Y-axis) are presented in bar graph form as means +/- SEM (n=5) for the indicated genes and genotypes in (A) male and (B) female mice. One-Way, unpaired ANOVA analysis with a Turkey multiple comparison test was used to calculate adjusted P values. Statistical significance of $P \leq 0.05$ (*) were considered significant.

3.9.7. Propionate Differentially Affects Hepatic GN mRNA Expression in a Sex-Specific Fashion that Requires VIP Signaling.

With the observation that a propionate diet was unsuccessful at elevating IGN mRNA gene expression, we next turned to the liver as it is the primary glucose producing organ. To that end, we repeated the dPCR measurements as described in figure 11 using hepatic tissue comparing mice fed a normal versus propionate diet. This study demonstrated that a propionate diet elevated mRNA gene expression in G6Pase and FBP1 in male WT mice, while downregulating these two genes and PCK1 in female WT mice (**Fig. 21**). Heterozygous and homozygous mutant VIP male and female mice lost statistical significance in their differentially regulated mRNA levels, suggesting that propionate's effect on hepatic GN expression is dependent upon VIP signaling. These data indicate that mice fed a propionate diet regulate hepatic GN mRNA expression in a similar, but not identical, manner to that of intestinal GN

mRNA expression in rats fed the same diet. Moreover, both species appear to depend on VIP signaling to bring about these mRNA expression changes.

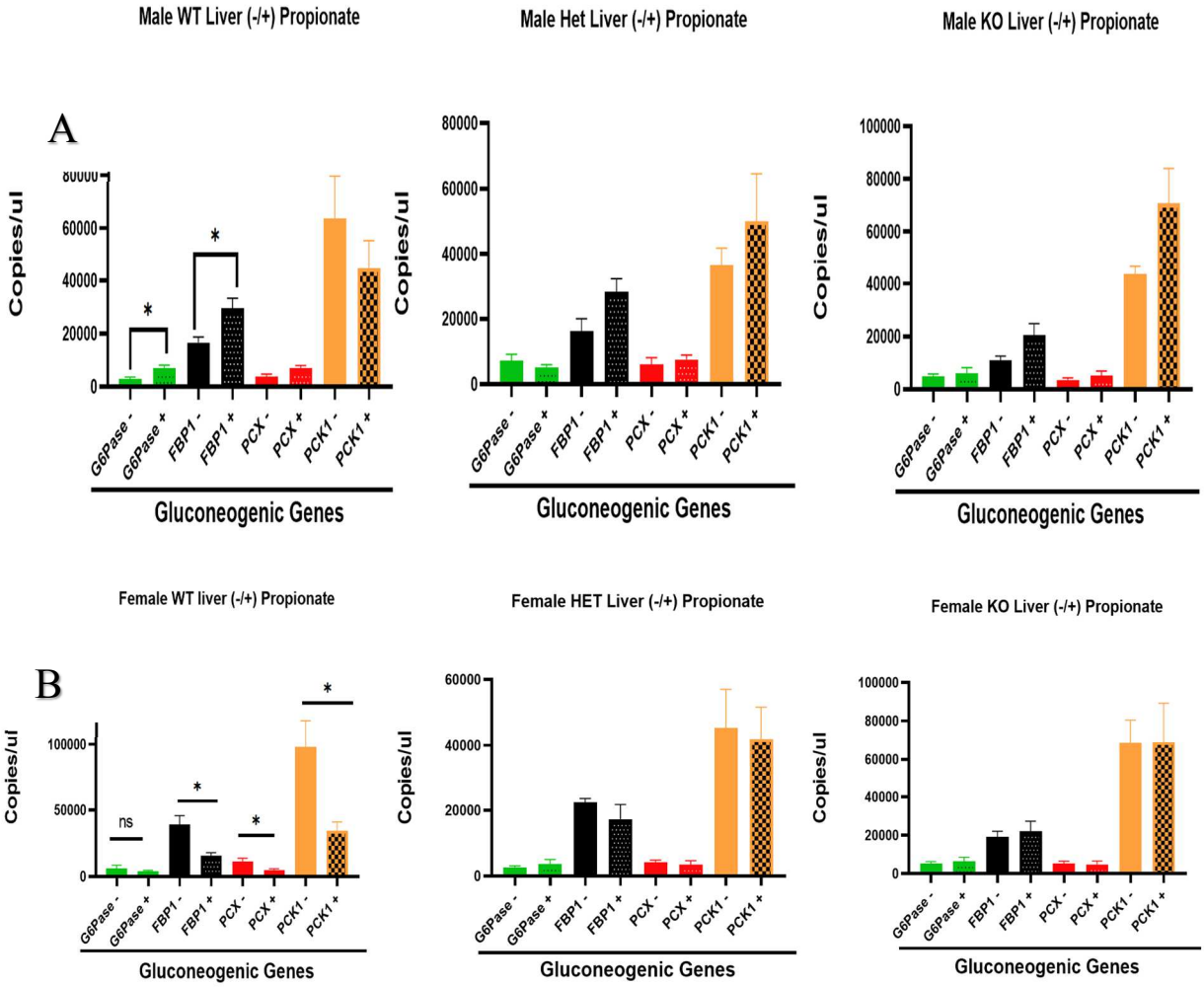

Figure 21. **Propionate Differentially Affects Hepatic GN mRNA Expression in a Sex-Specific Fashion that Requires VIP Signaling.** Absolute starting RNA template concentrations (Y-axis) are presented in bar graph form as means +/- SEM (n=5) for the indicated genes and genotypes in (A) male and (B) female mice. One-Way, unpaired ANOVA analysis with a Turkey multiple comparison test was used to calculate adjusted P values. Statistical significance of $P \leq 0.05$ (*) were considered significant.

3.10. Discussion

Our study confirmed mRNA expression for all four gluconeogenic genes in jejunum tissue of male and female VIP WT mice fed a standard diet. PCK1 exhibited significantly higher mRNA levels compared to the other three GN genes, while FBP1 mRNA was lowest. This IGN

expression profile was similar to that observed in hepatic tissue as PCK1 was expressed highest, with the other three genes expressed at lower mRNA levels. Interestingly, Females expressed lower intestinal GN mRNA expression, but greater hepatic GN expression compared to males. Previous studies have shown similar results (Dphil et al., 2005; Potts et al., 2018. However, no study to our knowledge has measured all four gluconeogenic genes from jejunum and liver tissue. We hypothesized that the mRNA expression of gluconeogenic genes from jejunum of VIP WT mice fed a propionate diet for two weeks would be elevated as reported by. De Vadder using rats fed a propionate diet (De Vadder et al., 2015) Surprisingly, our data did not support such a mechanism as we did not see any induction in intestinal GN mRNA expression due to a propionate diet. One possible explanation for this discrepancy could be that this study utilized rats that are not under similar regulatory control as that seen in mice (e.g., a species effect). These authors used exogenous VIP and a VPAC1 antagonist by intraperitoneal injection. Since VIP has a half-life of 1 min in blood, it is difficult to know whether the elevation of jejunum G6Pase enzymatic activity was caused by VIP acting on peritoneal versus intestinal cells. In a similar perspective, the cell inhibition that the VPAC1 antagonist is effecting is not known. To measure expression of all four gluconeogenic genes in mRNA level in jejunum and liver, our approach was to employ male and female VIP WT, HET, and KO mice. Our study showed that male and female WT mice fed propionate did not show elevated G6pase or other gluconeogenic gene mRNA levels, compared to control diet. Female, but not male, HET mice did exhibit elevated G6pase mRNA levels due to a propionate diet but did not reach statistical significance. An opposite trend was observed in male HET. VIP is negative inducer of G6Pase by propionate in female mice, while is it is a positive activator of G6Pase in mice fed a propionate diet. Previously, in 2013, De-Vadder reported that a propionate diet fed to male rats elevated jejunal

G6pase enzymatic activity and PCK1 mRNA expression. PCK1 expression was blunted when jejunum was treated with neurotoxin. In stark contrast, our experiments using mice resulted in opposite results. PCK1 mRNA expression levels went down in VIP HET and KO male mice, while in female mice its expression was elevated. PCX mRNA expression levels did not change due to VIP deficiency regardless of diet. With exception of VIP HET female and male, mRNA expression levels went up slightly in the presence of propionate but did not reach statistical significance. FBP1 is the only gluconeogenic gene that supported our hypothesis and showed the same mRNA expression in male and female, except for VIP WT female that failed to increase gene expression in the presence of propionate. Finally, female KO induced mRNA in the presence of propionate, but did not reach statistical significance. However, to get a better understanding, increasing the number of replicates is a major future goal.

One of the most interesting results demonstrated by this study was that PCK1 expression had completely opposite profiles in male and female mouse jejunum tissue, while in liver this gene had the same expression profile in both sexes due to VIP deficiency. In male jejunum, a propionate diet decreased the expression of PCK1 mRNA in VIP WT by about 2.5-fold, and the same level of reduction was seen in HET, and KO in the presence and absence of propionate. These results show that VIP is a positive regulatory influence of PCK1 in male jejunum tissue and propionate is an inhibitor of VIP. In female, VIP is a negative regulatory factor towards PCK1 mRNA expression. When VIP levels were reduced to half or HET, the expression of PCK1 increased by 50%, and the expression increased by 200% when VIP levels were completely knockout out (e.g., null). Propionate reduced this elevation by 50% in WT, Het and KO. As mentioned above, PCK1 expressed significantly higher mRNA levels than the other

three genes in jejunum of male and female mice, and PCK1 has other activities in intestine rather than gluconeogenesis.

According to our study, VIP and propionate do not have significant correlation, and propionate failed to upregulate mRNA levels of G6Pase, PCX and PCK1 in jejunum of male and female mice. Propionate has a well-established role in activation of IGN in rats.

The small intestine is made of three parts: duodenum, jejunum, and ileum. The first and shortest section of the intestine is duodenum, which receives digested food from the stomach, and plays an essential role in digesting food. The jejunum is the midsection of intestine that connects the duodenum to the ileum. The jejunum contains more villi and circular folds, which increase surface for absorption of digested nutrient particles from duodenum. Therefore, the jejunum is the main specialized section of intestine for nutrient absorption. Ileum is the last part of the intestine, and it absorbs vitamin B12, bile acid and other nutrients that were not absorbed within the jejunum (**See Fig. 22**).

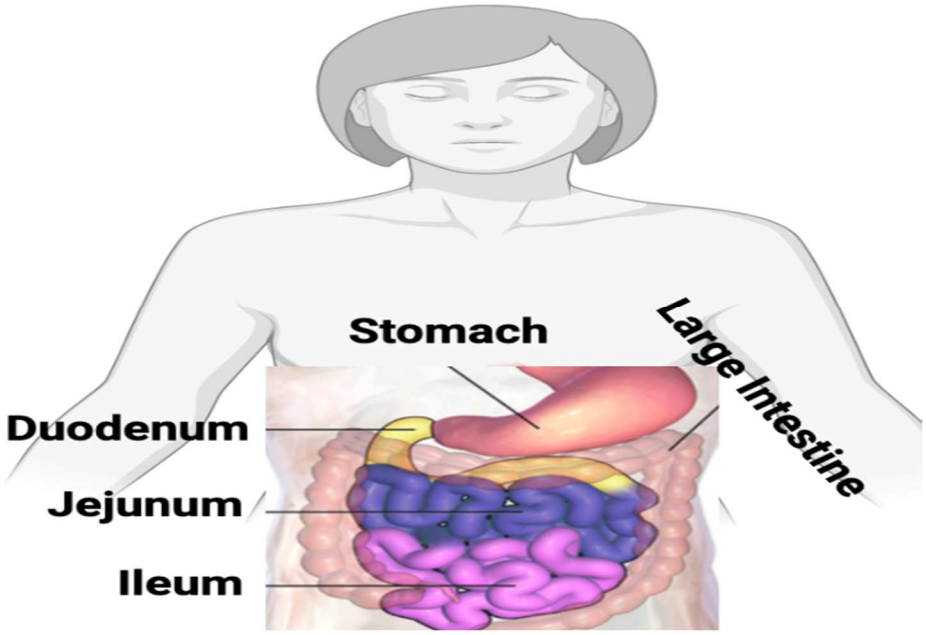

Figure 22. **Anatomy of the small intestines.**

The cross-section of the small intestine consists of four layers which are mucosa, submucosa, muscular layer, and adventitia. The mucosa section is made of epithelial cell and the main function of mucosa is absorption, transporting of nutrients, and protection of the body from foreign pathogens. Enterocytes are the main cell type of intestinal epithelial cells and has an essential role in absorption of ions, water, carbohydrate, peptides, and lipids. The other cells that are found are Goblet, Paneth, immune, and stem cells, but in smaller percentages compared to enterocytes cells (Kong et al., 2018;**Fig. 23**). It has been well established that the epithelial cells of intestine have a role in the activation of gluconeogenic genes. For our study, we used about 2.5 mm of whole jejunum tissue which composed of all four layers of intestine, not just epithelial cells. Therefore, the other three layers may contribute to IGN mRNA expression. One study reported using isolated bovine intestine epithelial cell (BIEC) line and measured the expression of PCK1, Fbp1, and PCX genes, which were elevated in response to propionate. However, G6pase mRNA expression was not affected by propionate in BIEC (Zhan et al.,2020).

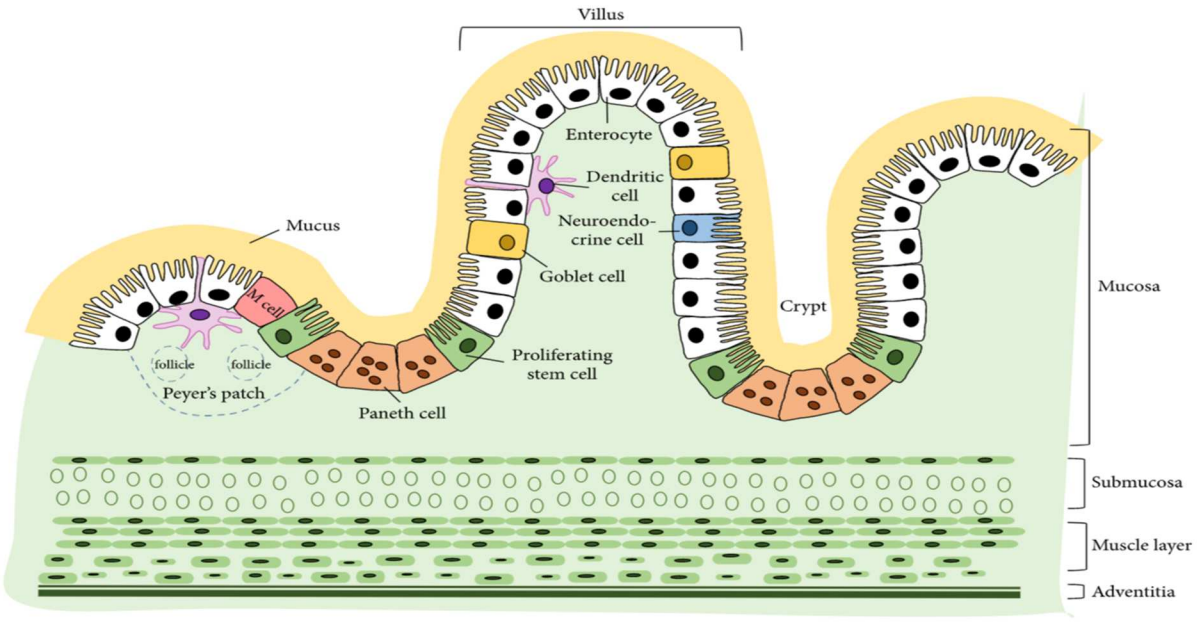

Figure 23. **Cross-section of small intestine shows the major cells that are found in mucosa section.** This carton image is taken from (Kong et al.,2018).

A novel function of G6Pase in glucose absorption was reported in the intestines of mice deficient for the glucose transporter 2 (GLUT2). Normally, glucose from the intestinal lumen enters the enterocyte through sodium linked glucose transporter 1 (SGLT1) on the brush border and releases into the blood via the GLUT2 facilitative glucose transporter. In the absence of GLUT2 transporter however, another transporter required G6Pase to help glucose transporting into the endoplasmic reticulum. is the authors concluded that glucose enters the enterocyte still via SGLT1, but is then is phosphorylated by hexokinase and diverted to the endoplasmic reticulum via a specific G6P transporter, for its eventual hydrolysis of its phosphate by G6Pase. Glucose product can then be released to the circulation (Stümpel et al., 2001). Our study showed that G6Pase mRNA expression levels in male mouse liver elevated in response to propionate, G6Pase is a nonspecific enzyme, which hydrolyzes many hexose phosphates such as mannose-6-phosphate. The hydrolyzing role of this enzyme is dependent on the presence of G-6 phosphate transporter on the endoplasmic reticulum. In human, the gene that encodes this transporter is expressed ubiquitously, and some tissues such as brain, heart and skeletal muscles contain the variant G-6 phosphate transporter that is produced by alternative splicing. For both transporters the variant and non-variant function as a G-6 phosphate transporter (G6PT) and have roles in maintaining glucose homeostasis (Lin B et al., 2000). G6pase activity in the small intestine is species specific and is dependent on feeding behavior habits. Previously, a research group examined G6Pase and the G6PT in liver, and intestine of rat, human, and guinea pig by mRNA, protein, and enzymatic activity. G6Pase and G6PT mRNA level in the small intestine and liver were varied within these different animals. In both human and guinea pig intestinal tissues, G6Pase mRNA levels were half of those expressed in the liver while rat intestinal G6pase mRNA levels were one fifth of the expression in liver. The expression levels of G6Pase and

G6PT were evaluated at the protein level. Like the data that was obtained from mRNA expression levels, both G6Pase and G6PT were expressed higher in the intestine of human and pig, but very low in intestine of rat. The protein expression level in intestine and liver of guinea pig was the same, but in human intestine the protein expression was 50% that of liver. The expression of G6Pase and G6PT in the intestinal microsomes isolated from rat was either very low or not detectable compared to protein expression in human and pig intestine The G6Pase activity in the liver and intestine microsomes from different species (rat, human, and guinea pig) were measured by produced glucose after the addition of the G6P substrate. In the livers of all three animals, G6Pase had high specific activity, while intestine of these animals had very low activity compared to the liver of human and pig, and no specific activity in rat intestine (Varga et al., 2019). However, De-Vadder showed that G6Pase activity was increased in response to propionate or VIP, and it was ablated with a VIP receptor antagonist. The G6Pase enzymatic activity was measured by adding the substrate G6P and non-substrate B- glycerol-phosphate to the sample and the inorganic phosphate was measured in both samples. It is hard to know from where the inorganic phosphate was released by G6Pase. Our results match well with Varga's lab results, which mRNA expression of G6Pase in intestine of male and female (average of male and female) is one fifth the expression in liver of mice (with exception that Varga lab used rat and our lab used mice model). G6Pase is the last step of gluconeogenesis pathway enzyme, and it is possible the glucose comes to the cell from stored glycogen by glycogenolysis and becomes phosphorated by a kinase enzyme. Before glucose goes down to the next step in glycolysis pathway, G6Pase will dephosphorylate the G-6-phosphate to glucose. It would take longer time to be regulated than the other three genes, or the half lifetime is longer than other three genes. Our lab also showed that G6pase enzymatic activity was upregulated in present of propionate

and absence of VIP or in VIP KO. Interestingly, when it came to investigate IGN, many research groups studied G6Pase enzyme as the representor of gluconeogenesis, especially in intestine regardless of sex. The expression of this gene is dependent on species, feeding behavior, transporter, diet, etc. (Varga et al., 2019).

Due to their low expression levels, little interest in FBP1 and PCX is apparent in the literature (Dphil, 2005) According to the gluconeogenic substrates that come from different sources, fructose-6-phosphate, which is the product of FBP1 enzyme, comes directly from diet and therefore in some occasions, there is no need for this enzyme. Under the role of glutamine as a substrate for the gluconeogenic pathway, PCX is not needed since this enzyme converts pyruvate to oxaloacetate (Fig 23). Most attentions were focused on the expression of G6Pase and PCK1 since these two enzymes are expressed predominantly in neonatal rats, mice, and rabbits in response to prolong fasting and/or diabetes. These two enzymes have other physiological roles beside their gluconeogenic roles.

Previously, the role of IGN was reported in a mice model during long-term fasting with deletion of the G6pase catalytic subunit (G6PC) in liver and with a combined deletion of the G6PC in liver and intestine. The blood glucose was compared during prolonged fasting in mice with a liver deletion of the G6pase catalytic (G6PC) and in mice with a combined deleting of the G6PC in liver and intestine. The plasma glucose concentration of the intestine and liver KO mice remained low (60 mg/dL) through the 48 h-fasting period. While the plasma glucose concentration of just liver KO mice was 90 mg/dL. This observation strongly supports the previous report on the role of kidney as approximately 70% and the intestine approximately 30% in providing glucose during an hepatic phase of liver transplantation in humans (Penhoat et al., 2013).

In one study reported by using the liver specific G6PC KO mice that mice were normoglycemic under standard diet and undergo a transient hypoglycemic episode under long-term fasting. It was due to the absence of liver gluconeogenic, but eventually reached to normal glycemia. This steady state is due to rapid activation of IGN therefore the liver is the first line organ for maintaining blood glycemia under normal diet. But once liver failed to maintain blood glycose due to not having enough substrates that come from diet or under transplantation, kidney and intestine are there to maintain normal glycemia (Mutel E et al., 2011). According to our study that G6Pase and other gluconeogenic genes in female liver did not response to propionate and propionate downregulated the expression of these genes in post-absorptive situation. This indicates that male and female metabolism is regulating differently and lots of research teams didn't differentiate the sex of animal model they used for their research. On the other hand, in male liver mice propionate upregulated the expression of these genes except of PCK1 gene and independent of VIP signaling. It would be very interesting result if repeat this study in prolong fasting situation and compared the result of liver and intestine with post-absorptive and prolong fasting situations. Metabolism is a very complicate system, and it is depending to species, diet, eating behavior, mood, genetic, and hormone. Gluconeogenic genes have other functions beside their gluconeogenic function, therefore, the IGN investigation needs to evaluate not just in mRNA level but also the glycogen content, transporters of these genes, blood glucose and so one. Gluconeogenic pathway has different substrates, and those substrates can come in at any steps from different sources which would just need one or two of these enzymes to produce glucose by gluconeogenic pathway (**See Fig. 24**).

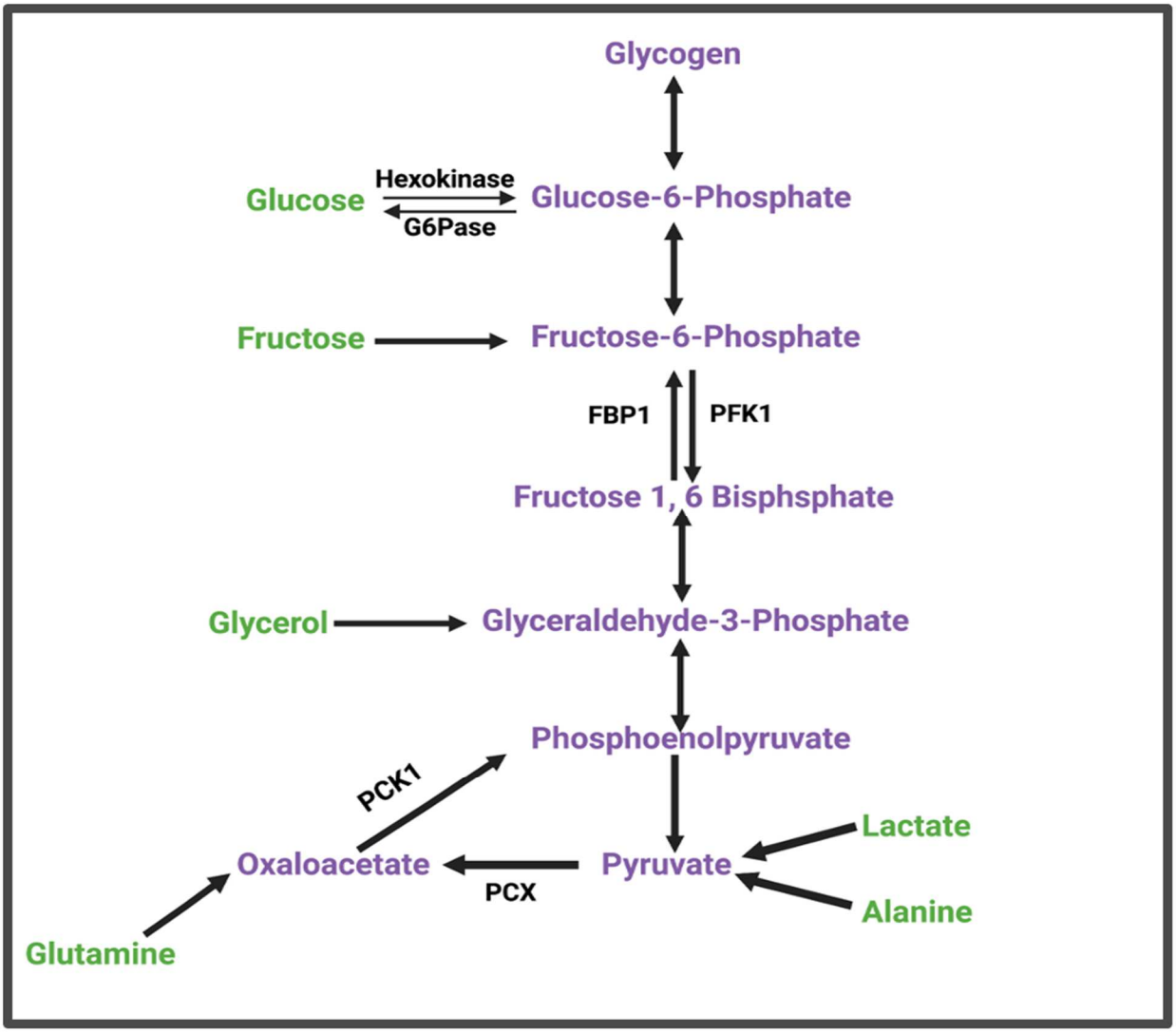

Figure 24. **Gluconeogenic pathway** with its four significant enzymes and different substrate that come from different source are showing in green.

PCK1 highly expresses in the liver and kidney however according to our study result it expresses 31-fold less in the jejunum than in liver. Although PCK1 is a gluconeogenic enzyme, it also plays a cataplerotic role in fatty acid esterification, AA metabolism, and TCA maintenance. In a small intestine, PCK1 KO mice were measured of glucose homeostasis, lipid absorption, AA metabolism and energy homeostasis. However, small intestine PCK1 KO mice demonstrated that intestinal PCK1 is not necessary for normal glucose production nor does its loss protect glucose production during type 1 diabetes or diet induced obesity. In other hand, small intestine PCK1

mild impairment in dietary lipid absorption and secretion, altered AA profiles and impaired AA catabolism, and elevated TCA cycle intermediates and changed intestinal redox state (Potts et, al., 2018). Consequently, the PCK1 pathway in the small intestine play multiple roles by facilitating glucose production, lipide absorption and secretion, and AAA catabolism. Our study result showed that in male and female jejunum propionate reduced expression of PCK1, so this indicates the probably of propionate activated other pathways rather than activation of PCK1.

I summary, propionate failed to induce gluconeogenic genes in the jejunum of male or female mice. However, propionate upregulated the expression of these genes in male liver. VIP signaling is however required for propionate-influences in three hepatic gluconeogenic genes (FBP1, PCX, and PCK1). And VIP is also positive regulatory for male jejunum PKC1 and PBP1 genes in jejunum of both sexes. All four-gluconeogenesis genes had different expression profiles in liver and jejunum of both sexes.

The liver and kidney are the primary organs that regulate endogenous glucose production (EGP) by the gluconeogenesis pathway. There are, however, other organs like the intestines that also express all four gluconeogenic genes, yet it is unclear as to the biological role they are playing. There are several possible roles for these gluconeogenic enzymes in the intestines. One mechanism is thought to be a cataplerotic pathway that results in the exportation of metabolites from the TCA cycle, thus balancing anaplerotic pathways that input metabolites into the TCA cycle, such as catabolic amino acid and fatty-acid metabolisms. A second cataplerotic pathway is gluconeogenesis as the intestines in rats can produce up to 17% of fasting EGP. In contrast, mice lacking the gluconeogenic enzyme, PEP carboxykinase, did not influence glycemia, even when the mice were chemically induced to a diabetic state with streptozotocin.

3.11. Future Studies

In the future, our plan is to measure FBP1 protein expression from jejunum and liver tissues by Western analysis. Male and female mice from all four groups on both diets will be used. We expect to observe elevated FBP1 protein from mice on propionate diets in VIP KO versus WT littermates. Next we will measure the enzymatic activity of FBP1. Lastly, we will purify intestinal epithelial cells from jejunum tissue and measure mRNA, protein and enzymatic activity levels for the four gluconeogenic genes by dPCR, Western blot and enzymatic assays.

REFERENCES

Avila, C., Holloway, A.C., Hahn, M.K. et al. An Overview of Links Between Obesity and Mental Health. Curr Obes Rep 4, 303–310 (2015). https://doi.org/10.1007/s13679-015-0164-9 .

Anderson P, Gonzalez-Rey E. Vasoactive intestinal peptide induces cell cycle arrest and regulatory functions in human T cells at multiple levels. Mol Cell Biol. 2010 May;30(10):2537-51. doi: 10.1128/MCB.01282-09. Epub 2010 Mar 15. PMID: 20231362; PMCID: PMC2863702

Bains M, Laney C, Wolfe AE, Orr M, Waschek JA, Ericsson AC, Dorsam GP. Vasoactive Intestinal Peptide Deficiency Is Associated With Altered Gut Microbiota Communities in Male and Female C57BL/6 Mice. Front Microbiol. 2019 Dec 2;10:2689. doi: 10.3389/fmicb.2019.02689. PMID: 31849864; PMCID: PMC6900961.

Buss C, Davis EP, Shahbaba B, Pruessner JC, Head K, Sandman CA. Maternal cortisol over the course of pregnancy and subsequent child amygdala and hippocampus volumes and affective problems. Proc Natl Acad Sci U S A. 2012 May 15;109(20):E1312-9. doi: 10.1073/pnas.1201295109. Epub 2012 Apr 23. PMID: 22529357; PMCID: PMC3356611.

Cao L, Cui X, Hu J, Li Z, Choi JR, Yang Q, Lin M, Ying Hui L, Xu F. Advances in digital polymerase chain reaction (dPCR) and its emerging biomedical applications. Biosens Bioelectron. 2017 Apr 15;90:459-474. doi: 10.1016/j.bios.2016.09.082. Epub 2016 Sep 25. PMID: 27818047.

Chadio S, Kotsampasi B. The role of early life nutrition in programming of reproductive function. J Dev Orig Health Dis. 2014 Feb;5(1):2-15. doi: 10.1017/S204017441300038X. PMID: 24847686.

Ceraudo E, Murail S, Tan YV, Lacapère JJ, Neumann JM, Couvineau A, Laburthe M. The vasoactive intestinal peptide (VIP) alpha-Helix up to C terminus interacts with the N-terminal ectodomain of the human VIP/Pituitary adenylate cyclase-activating peptide 1 receptor: photoaffinity, molecular modeling, and dynamics. Mol Endocrinol. 2008 Jan;22(1):147-55. doi: 10.1210/me.2007-0361. Epub 2007 Sep 20. PMID: 17885205; PMCID: PMC5419634.

Colwell CS, Michel S, Itri J, Rodriguez W, Tam J, Lelievre V, Hu Z, Liu X, Waschek JA. Disrupted circadian rhythms in VIP- and PHI-deficient mice. Am J Physiol Regul Integr Comp Physiol. 2003 Nov;285(5):R939-49. doi: 10.1152/ajpregu.00200.2003. Epub 2003 Jul 10. PMID: 12855416.

Couvineau A, Laburthe M. VPAC receptors: structure, molecular pharmacology and interaction with accessory proteins. Br J Pharmacol. 2012 May;166(1):42-50. doi: 10.1111/j.1476-5381.2011.01676.x. PMID: 21951273; PMCID: PMC3415636.

D. Witters, B. Sun, S. Begolo, J. Rodriguez-Manzano, W. Robles, R.F. Ismagilov
Lab Chip, 14 (2014), pp. 3225-3232

De Vadder F, Kovatcheva-Datchary P, Goncalves D, Vinera J, Zitoun C, Duchampt A, Bäckhed F, Mithieux G. Microbiota-generated metabolites promote metabolic benefits via gut-brain neural circuits. Cell. 2014 Jan 16;156(1-2):84-96. doi: 10.1016/j.cell.2013.12.016. Epub 2014 Jan 9. PMID: 24412651.

De Vadder F, Plessier F, Gautier-Stein A, Mithieux G. Vasoactive intestinal peptide is a local mediator in a gut-brain neural axis activating intestinal gluconeogenesis. Neurogastroenterol Motil. 2015 Mar;27(3):443-8. doi: 10.1111/nmo.12508. Epub 2015 Jan 13. PMID: 25586379.

Delgado M, Gonzalez-Rey E, Ganea D. VIP/PACAP preferentially attract Th2 effectors through differential regulation of chemokine production by dendritic cells. FASEB J. 2004 Sep;18(12):1453-5. doi: 10.1096/fj.04-1548fje. Epub 2004 Jul 1. PMID: 15231725.

Dethlefsen L, Eckburg PB, Bik EM, Relman DA. Assembly of the human intestinal microbiota. Trends Ecol Evol. 2006 Sep;21(9):517-23. doi: 10.1016/j.tree.2006.06.013. Epub 2006 Jul 3. PMID: 16820245.

Dorsam GP, Benton K, Failing J, Batra S. Vasoactive intestinal peptide signaling axis in human leukemia. World J Biol Chem. 2011 Jun 26;2(6):146-60. doi: 10.4331/wjbc.v2.i6.146. PMID: 21765981; PMCID: PMC3135862.

Fabricius D, Karacay B, Shutt D, Leverich W, Schafer B, Takle E, Thedens D, Khanna G, Raikwar S, Yang B, Desmond ME, O'Dorisio MS. Characterization of intestinal and pancreatic dysfunction in VPAC1-null mutant mouse. Pancreas. 2011 Aug;40(6):861-71. doi: 10.1097/MPA.0b013e318214c783. PMID: 21697765.

Francesca Cirulli, Chiara Musillo, Alessandra Berry,
Maternal Obesity as a Risk Factor for Brain Development and Mental Health in the Offspring,Neuroscience,Volume 447,2020,Pages 122-135,SSN 0306-4522,
Https://doi.org/10.1016/j.neuroscience.2020.01.023.
(https://www.sciencedirect.com/science/article/pii/S0306452220300439)

F Rajas, M Croset, C Zitoun, S Montano, G Mithieux; Induction of PEPCK gene expression in insulinopenia in rat small intestine. Diabetes 1 July 2000; 49 (7): 1165–1168.

Gautier-Stein, A., Rajas, F., & Mithieux, G. (2021). Intestinal gluconeogenesis and protein diet: Future directions. *Proceedings of the Nutrition Society, 80*(2), 118-125. doi:10.1017/S0029665120007922

Gaw AJ, Aberdeen J, Humphrey PP, Wadsworth RM, Burnstock G. Relaxation of sheep cerebral arteries by vasoactive intestinal polypeptide and neurogenic stimulation: inhibition by L-NG-monomethyl arginine in endothelium-denuded vessels. Br J Pharmacol. 1991 Mar;102(3):567-72. doi: 10.1111/j.1476-5381.1991.tb12213.x. PMID: 1364820; PMCID: PMC1917941.

Grant S, Lutz EM, McPhaden AR, Wadsworth RM. Location and function of VPAC1, VPAC2 and NPR-C receptors in VIP-induced vasodilation of porcine basilar arteries. J Cereb Blood Flow Metab. 2006 Jan;26(1):58-67. doi: 10.1038/sj.jcbfm.9600163. PMID: 15959462.

Jayawardena D, Anbazhagan AN, Guzman G, Dudeja PK, Onyuksel H. Vasoactive Intestinal Peptide Nanomedicine for the Management of Inflammatory Bowel Disease. *Mol Pharm*. 2017;14(11):3698-3708. doi:10.1021/acs.molpharmaceut.7b00452.

Hassan M, Refai E, Andersson M, Schnell PO, Jacobsson H. In vivo dynamical distribution of 131I-VIP in the rat studied by gamma-camera. Nucl Med Biol. 1994 Aug;21(6):865-72. doi: 10.1016/0969-8051(94)90166-x. PMID: 9234336.

Hassan M, Refai E, Andersson M, Schnell PO, Jacobsson H. In vivo dynamical distribution of 131I-VIP in the rat studied by gamma-camera. Nucl Med Biol. 1994 Aug;21(6):865-72. doi: 10.1016/0969-8051(94)90166-x. PMID: 9234336.

Hashimoto H, Nishino A, Shintani N, Hagihara N, Copeland NG, Jenkins NA, Yamamoto K, Matsuda T, Ishihara T, Nagata S, Baba A. Genomic organization and chromosomal location of the mouse vasoactive intestinal polypeptide 1 (VPAC1) receptor. Genomics. 1999 May 15;58(1):90-3. doi: 10.1006/geno.1999.5805. PMID: 10331949.

Harmar AJ, Marston HM, Shen S, Spratt C, West KM, Sheward WJ, Morrison CF, Dorin JR, Piggins HD, Reubi JC, Kelly JS, Maywood ES, Hastings MH. The VPAC(2) receptor is essential for circadian function in the mouse suprachiasmatic nuclei. Cell. 2002 May 17;109(4):497-508. doi: 10.1016/s0092-8674(02)00736-5. PMID: 12086606.

Hirabayashi T, Nakamachi T, Shioda S. Discovery of PACAP and its receptors in the brain. J Headache Pain. 2018 Apr 4;19(1):28. doi: 10.1186/s10194-018-0855-1. PMID: 29619773; PMCID: PMC5884755.

Hokari R, Lee H, Crawley SC, Yang SC, Gum JR Jr, Miura S, Kim YS. Vasoactive intestinal peptide upregulates MUC2 intestinal mucin via CREB/ATF1. Am J Physiol Gastrointest Liver Physiol. 2005 Nov;289(5):G949-59. doi: 10.1152/ajpgi.00142.2005. PMID: 16227528.

Ishihara T, Shigemoto R, Mori K, Takahashi K, Nagata S. Functional expression and tissue distribution of a novel receptor for vasoactive intestinal polypeptide. Neuron. 1992 Apr;8(4):811-9. doi: 10.1016/0896-6273(92)90101-i. PMID:314625.

Kong S, Zhang YH, Zhang W. Regulation of Intestinal Epithelial Cells Properties and Functions by Amino Acids. Biomed Res Int. 2018 May 9;2018:2819154. doi: 10.1155/2018/2819154. PMID: 29854738; PMCID: PMC5966675.

Laburthe M, Couvineau A, Tan V. Class II G protein-coupled receptors for VIP and PACAP: structure, models of activation and pharmacology. Peptides. 2007 Sep;28(9):1631-9. doi: 10.1016/j.peptides.2007.04.026. Epub 2007 May 22. PMID: 17574305.

Lelievre V, Favrais G, Abad C, Adle-Biassette H, Lu Y, Germano PM, Cheung-Lau G, Pisegna JR, Gressens P, Lawson G, Waschek JA. Gastrointestinal dysfunction in mice with a targeted mutation in the gene encoding vasoactive intestinal polypeptide: a model for the study of intestinal ileus and Hirschsprung's disease. Peptides. 2007 Sep;28(9):1688-99. doi: 10.1016/j.peptides.2007.05.006. Epub 2007 May 18. PMID: 17606312; PMCID: PMC2042583.

Lorenz TC. Polymerase chain reaction: basic protocol plus troubleshooting and optimization strategies. J Vis Exp. 2012 May 22;(63):e3998. doi: 10.3791/3998. PMID: 22664923; PMCID: PMC4846334.

Lin B, Pan CJ, Chou JY. Human variant glucose-6-phosphate transporter is active in microsomal transport. Hum Genet. 2000 Nov;107(5):526-9. doi: 10.1007/s004390000404. PMID: 11140953.

Mithieux, Gillesa,b,c,d; Andreelli, Fabrizioe,f,g; Magnan, Christopheg,h Intestinal gluconeogenesis: key signal of central control of energy and glucose homeostasis, Current Opinion in Clinical Nutrition and Metabolic Care: July 2009 - Volume 12 - Issue 4 - p 419-423doi: 10.1097/MCO.0b013e32832c4d6a

Morley AA. Digital PCR: A brief history. Biomol Detect Quantif. 2014 Aug 15;1(1):1-2. doi: 10.1016/j.bdq.2014.06.001. PMID: 27920991; PMCID: PMC5129430.

Mutel E, Gautier-Stein A, Abdul-Wahed A, Amigó-Correig M, Zitoun C, Stefanutti A, Houberdon I, Tourette JA, Mithieux G, Rajas F. Control of blood glucose in the absence of hepatic glucose production during prolonged fasting in mice: induction of renal and intestinal gluconeogenesis by glucagon. Diabetes. 2011 Dec;60(12):3121-31. doi: 10.2337/db11-0571. Epub 2011 Oct 19. PMID: 22013018; PMCID: PMC3219939.

Neish AS. Microbes in gastrointestinal health and disease. Gastroenterology. 2009 Jan;136(1):65-80. doi: 10.1053/j.gastro.2008.10.080. Epub 2008 Nov 19. PMID: 19026645; PMCID: PMC2892787.

Nicole P, Du K, Couvineau A, Laburthe M. Site-directed mutagenesis of human vasoactive intestinal peptide receptor subtypes VIP1 and VIP2: evidence for difference in the structure-function relationship. J Pharmacol Exp Ther. 1998 Feb;284(2):744-50. PMID: 9454823.

Nussbaum, J., Van Dyken, S., von Moltke, J. *et al.* Type 2 innate lymphoid cells control eosinophil homeostasis. *Nature* **502**, 245–248 (2013). https://doi.org/10.1038/nature12526

Nyberg B, Angelin B, Einarsson K. Somatostatin does not block the effect of vasoactive intestinal peptide on bile secretion in man. Eur J Clin Invest. 1992 Jan;22(1):60-6. doi: 10.1111/j.1365-2362.1992.tb01937.x. PMID: 1348475.

Ockerman PA. Glucose-6-phosphatase in human jejunal mucosa properties demonstrating the specific character of the enzyme activity. Biochim Biophys Acta. 1965 Jul 29;105(1):22-33. PMID: 4284996.

Oh KJ, Han HS, Kim MJ, Koo SH. Transcriptional regulators of hepatic gluconeogenesis. Arch Pharm Res. 2013 Feb;36(2):189-200. doi: 10.1007/s12272-013-0018-5. Epub 2013 Jan 30. PMID: 23361586.

Penhoat A, Fayard L, Stefanutti A, Mithieux G, Rajas F. Intestinal gluconeogenesis is crucial to maintain a physiological fasting glycemia in the absence of hepatic glucose production in mice. Metabolism. 2014 Jan;63(1):104-11. doi: 10.1016/j.metabol.2013.09.005. Epub 2013 Oct 14. PMID: 24135501.

Penhoat A, Fayard L, Stefanutti A, Mithieux G, Rajas F. Intestinal gluconeogenesis is crucial to maintain a physiological fasting glycemia in the absence of hepatic glucose production in mice. Metabolism. 2014 Jan;63(1):104-11. doi: 10.1016/j.metabol.2013.09.005. Epub 2013 Oct 14. PMID: 24135501.

Potts A, Uchida A, Deja S, Berglund ED, Kucejova B, Duarte JA, Fu X, Browning JD, Magnuson MA, Burgess SC. Cytosolic phosphoenolpyruvate carboxykinase as a cataplerotic pathway in the small intestine. Am J Physiol Gastrointest Liver Physiol. 2018 Aug 1;315(2):G249-G258. doi: 10.1152/ajpgi.00039.2018. Epub 2018 Apr 6. PMID: 29631378; PMCID: PMC6139646.

Rajas F, Bruni N, Montano S, Zitoun C, Mithieux G. The glucose-6 phosphatase gene is expressed in human and rat small intestine: regulation of expression in fasted and diabetic rats. Gastroenterology. 1999 Jul;117(1):132-9. doi: 10.1016/s0016-5085(99)70559-7. PMID: 10381919.

Said SI, Mutt V. Potent peripheral and splanchnic vasodilator peptide from normal gut. Nature. 1970 Feb 28;225(5235):863-4. doi: 10.1038/225863a0. PMID: 5415118.

Saiki RK, Gelfand DH, Stoffel S, Scharf SJ, Higuchi R, Horn GT, Mullis KB, Erlich HA. Primer-directed enzymatic amplification of DNA with a thermostable DNA polymerase. Science. 1988 Jan 29;239(4839):487-91. doi: 10.1126/science.2448875. PMID: 2448875.

Sherwood NM, Krueckl SL, McRory JE. The origin and function of the pituitary adenylate cyclase-activating polypeptide (PACAP)/glucagon superfamily. Endocr Rev. 2000 Dec;21(6):619-70. doi: 10.1210/edrv.21.6.0414. PMID: 11133067.

Stümpel F, Burcelin R, Jungermann K, Thorens B. Normal kinetics of intestinal glucose absorption in the absence of GLUT2: evidence for a transport pathway requiring glucose phosphorylation and transfer into the endoplasmic reticulum. Proc Natl Acad Sci U S A. 2001 Sep 25;98(20):11330-5. doi: 10.1073/pnas.211357698. Epub 2001 Sep 18. PMID: 11562503; PMCID: PMC58729.

Sutherland EW, Rall TW 1958. Fractionation and characterization of a cyclic adenine ribonucleotide formed by tissue particles. *J Biol Chem* 232: 1077–1091

Toscano MG, Delgado M, Kong W, Martin F, Skarica M, Ganea D. Dendritic cells transduced with lentiviral vectors expressing VIP differentiate into VIP-secreting tolerogenic-like DCs. Mol Ther. 2010 May;18(5):1035-45. doi: 10.1038/mt.2009.293. Epub 2010 Jan 12. PMID: 20068554; PMCID: PMC2890107.

Usdin TB, Bonner TI, Mezey E. Two receptors for vasoactive intestinal polypeptide with similar specificity and complementary distributions. Endocrinology. 1994 Dec;135(6):2662-80. doi: 10.1210/endo.135.6.7988457. PMID: 7988457.

Van Geldre LA, Lefebvre RA. Interaction of NO and VIP in gastrointestinal smooth muscle relaxation. Curr Pharm Des. 2004;10(20):2483-97. doi: 10.2174/1381612043383890. PMID: 15320758.

Varga V, Murányi Z, Kurucz A, Marcolongo P, Benedetti A, Bánhegyi G, Margittai É. Species-Specific Glucose-6-Phosphatase Activity in the Small Intestine-Studies in Three Different Mammalian Models. Int J Mol Sci. 2019 Oct 11;20(20):5039. doi: 10.3390/ijms20205039. PMID: 31614497; PMCID: PMC6829527.

Vertongen P, Solano RM, Juarranz MG, Perret J, Waelbroeck M, Robberecht P. Proline residue 280 in the second extracellular loop (EC2) of the VPAC2 receptor is essential for the receptor structure. Peptides. 2001 Sep;22(9):1363-70. doi: 10.1016/s0196-9781(01)00476-4. PMID: 11514016.

Vogelstein B, Kinzler KW. Digital PCR. Proc Natl Acad Sci U S A. 1999 Aug 3;96(16):9236-41. doi: 10.1073/pnas.96.16.9236. PMID: 10430926; PMCID: PMC17763.

Wu Y, Tang L, Wang B, Sun Q, Zhao P, Li W. The role of autophagy in maintaining intestinal mucosal barrier. J Cell Physiol. 2019 Nov;234(11):19406-19419. doi: 10.1002/jcp.28722. Epub 2019 Apr 24. PMID: 31020664.

Wu X, Conlin VS, Morampudi V, Ryz NR, Nasser Y, Bhinder G, Bergstrom KS, Yu HB, Waterhouse CC, Buchan AM, Popescu OE, Gibson WT, Waschek JA, Vallance BA, Jacobson K. Vasoactive intestinal polypeptide promotes intestinal barrier homeostasis and protection against colitis in mice. PLoS One. 2015 May 1;10(5):e0125225. doi: 10.1371/journal.pone.0125225. PMID: 25932952; PMCID: PMC4416880.

Watford M. Is the small intestine a gluconeogenic organ. Nutr Rev. 2005 Oct;63(10):356-60. doi: 10.1111/j.1753-4887.2005.tb00114.x. PMID: 16295149.

Ward ZJ, Bleich SN, Long MW, Gortmaker SL (2021) Association of body mass index with health care expenditures in the United States by age and sex. PLoS ONE 16(3): e0247307. https://doi.org/10.1371/journal.pone.0247307.

Xie X, Geng C, Li X, Liao J, Li Y, Guo Y, Wang C. Roles of gastrointestinal polypeptides in intestinal barrier regulation. Peptides. 2022 May;151:170753. doi: 10.1016/j.peptides.2022.170753. Epub 2022 Jan 31. PMID: 35114316.

Zhan K, Yang TY, Chen Y, Jiang MC, Zhao GQ. Propionate enhances the expression of key genes involved in the gluconeogenic pathway in bovine intestinal epithelial cells. J Dairy Sci. 2020 Jun;103(6):5514-5524. doi: 10.3168/jds.2019-17309. Epub 2020 Apr 8. PMID: 32278554.